# Materials & Design


## Topological Design of Pentamode Lattice Metamaterials Using A Ground Structure Method

--Manuscript Draft--

| | |
|---|---|
| **Manuscript Number:** | JMADE-D-20-03993R1 |
| **Article Type:** | Research Paper |
| **Keywords:** | Pentamode metamaterials;  Micro lattice;  Orthotropic symmetry;  Topology optimization;  Ground structure method |
| **Corresponding Author:** | ZHEN LUO, Ph.D.<br>University of Technology, Sydney<br>Sydney, AUSTRALIA |
| **First Author:** | Zuyu Li |
| **Order of Authors:** | Zuyu Li |
| | ZHEN LUO, Ph.D. |
| | Laichang Zhang, PhD |
| | Chun-Hui Wang, PhD |
| **Abstract:** | Pentamode metamaterials are a new class of artificially engineering three-dimensional lattice composites. There exist a few types of pentamode metamaterials that are dominated by ad hoc design motifs, while a systematic design approach is still missing. This paper will present an efficient topological optimization methodology to discover a series of novel pentamode lattice microarchitectures over a range of effective material properties. Firstly, the necessary and sufficient condition that is required for elasticity constants of pentamode micro lattices with at least elastically orthotropic symmetry is derived. Secondly, a general mathematical formulation for design optimization of such pentamode micro lattices is developed. Thirdly, a truss-based three-dimensional ground structure with geometrically orthotropic symmetry is generated, with geometric constraints to avoid intersection and overlap of truss bars within the ground structure. The genetic algorithm is then used to solve the topology optimization problem described by the ground structure. Finally, twenty-four pentamode lattices are designed to demonstrate the effectiveness of the proposed method. |
| **Response to Reviewers:** | The "Detailed Response to Reviewers" has been attached with the submission as an individual document. Thanks |

# Topological Design of Pentamode Lattice Metamaterials Using A Ground Structure Method

Zuyu Li [a], Zhen Luo [a,*], Lai-Chang Zhang [b], Chun-Hui Wang [c]

[a] School of Mechanical and Mechatronic Engineering
University of Technology Sydney, Sydney, NSW 2007, Australia
*( [*]Corresponding authors: zhen.luo@uts.edu.au, A/Prof Zhen Luo)*

[b] School of Engineering
Edith Cowan University, Perth, WA 6027, Australia

[c] School of Mechanical and Manufacturing Engineering
University of New South Wales, Sydney, NSW 2052, Australia

---

12 Nov 2020

Dear Editor

I am pleased to submit an original research article entitled [ "Topological Design of Pentamode Lattice Metamaterials Using A Ground Structure Method"] for consideration of publication in Materials & Design.

We believe that this manuscript is appropriate for publication by Materials & Design because this manuscript is exactly on rational design of novel pentamode metamaterial lattices using a new topology optimization method and prototyped by using appropriate additive manufacturing techniques.

This manuscript has not been published and is not under consideration for publication elsewhere. We have no conflicts of interest to disclose. If you feel that the manuscript is appropriate for your journal, we may suggest the following reviewers for your consideration:

[Prof. Fengwen Wang, email: fwan@mek.dtu.dk, Denmark Technical University]
[Prof. Yiqiang Wang, email: wangyq@dlut.edu.cn, Dalian University of Technology]
[Prof. Yan Huang, email: huangyan0725@stu.xjtu.edu.cn, Xi'an Jiaotong University]

Thank you for your consideration!

Sincerely,

Jeff

---

**Zhen (Jeff) Luo, PhD**
Associate Professor in Mechanical Engineering
School of Mechanical and Mechatronic Engineering
The University of Technology Sydney (UTS)
15 Broadway, Ultimo, NSW 2007, Australia.
Tel: (+61) 2 9514 2994
Fax: (+61) 2 9514 2655
Email: Zhen.luo@uts.edu.au

Graphical Abstract

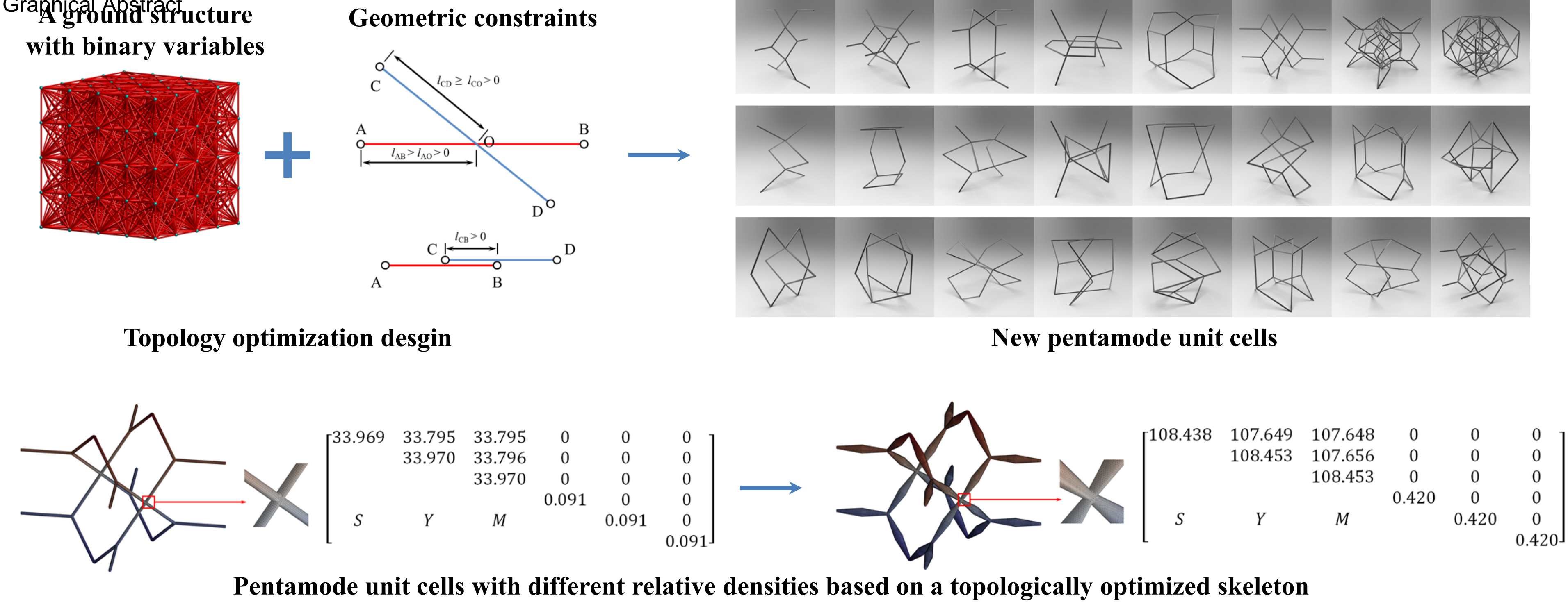

**Highlights**

- A general mathematical formulation is proposed for design of three-dimensional pentamode metamaterials with at least orthotropic symmetry.
- A ground-structure topology optimization method with the genetic algorithm is proposed for inverse design of pentamode lattices.
- Geometric constraints on intersection and overlap of bars are imposed on design optimization of truss-like lattices.
- Twenty-four new pentamode lattices are discovered, including isotropic, transverse isotropic and orthotropic.

# Response to Reviewers

Ms. Ref. No.: JMADE-D-20-03993

Title: Topological Design of Pentamode Lattice Metamaterials Using A Ground Structure Method

**Reviewer #1:**

The main objective of this paper is to use the genetic-algorithm-based ground structure method to design the pentamode metamaterials with at least orthotropic symmetry. The main works include the derivation of the necessary and sufficient condition required for elasticity matrices of pentamode metamaterials with at least orthotropic symmetry, and the definition of the optimization model. And then, some examples were given. However, the persuasive and comparative conclusions weren't drawn from the optimal results. There are some questions and comments as follows.

*(1) Authors proposed the topology optimization method to discover novel pentamode metamaterial lattices with at least orthotropic symmetry. Could it be applied for the anisotropic pentamode metamaterials? Sincere authors mentioned the anisotropic pentamode metamaterials in the introduction, it could be necessary to further discuss the application problem of the authors' method.*

**Reply:**

Thanks. At this stage, the proposed methodology has not applied to design fully anisotropic pentamode metamaterials, but it is not a limitation of the proposed topology optimization approach itself. The method is general and appliable to many different designs. It is the complexity of deriving the necessary and sufficient condition in theory that restrains the application of the proposed method to the fully anisotropic metamaterials. Once such a condition is derived, the topological optimization method developed in this paper can be used to find fully anisotropic pentamode unit cells. We are currently working on it. However, at least, we consider the current work as an important advance compared with the recent references that only focused on isotropic pentamode unit cells (e.g. [21] and [22] in 2019), since it can find a range of transverse isotropic and orthotropic pentamode unit cells and significantly broaden the family of pentamode lattices. We have added this discussion in the Conclusions of the revised paper.

*(2) To find the necessary and sufficient condition for this characteristic polynomial Eq. (2) to have only one non-zero root, authors chose the second case that at least one of 11, 22 and 33 is positive and mentioned that it is more complicated and physically meaningful. After the derivation, authors should clarify this point and detailedly explain that the non-zero eigenvalue = 11 + 22 + 33 is not always proportional to the bulk modulus, and the eigenvector in Eq (16) does not always correspond to hydrostatic pressure either. Therefore, ones can naturally accept the conclusion that a relatively very large ratio of the bulk modulus to the shear modulus is no more a sufficient condition for non-isotropic pentamode metamaterials.*

**Reply:**

Thanks for the suggestion. We have given more details in explaining this issue after Eq. (16).

*(3) Genetic algorithm has been used to solve topology optimization problems. Its merits and drawbacks were pointed out in section 3.2. It is not essential. Generally, we introduce the used algorithm principle in the*

*separate section.*

**Reply:**

Thanks for the suggestion. We have added a simple introduction of the genetic algorithm principle in Section 3.2 now. It is noted that we just use the Matlab built-in function to implement the classical genetic algorithm, and this paper will not effort to improve the genetic algorithm itself. The main purpose of this section is to emphasize that for the discrete optimization problem with relatively small-scale, the genetic algorithm can be used as an appropriate optimization solver, instead of using mathematical programming methods as used in most topology optimization problems.

*(4) In the generation of the ground structure, how to determine the number of bars and design variables and the fully connected ground structure? Could the concrete computing process be listed?*

**Reply:**

We have provided Matlab scripts online for free download and use for research. The Web link and introduction are given in Section 3.3. The scripts can generate the proposed ground structures and determine which bars are active according to the given design variables. The numbers of Cartesian mesh nodes are chosen as user-input values to generate simple or complex ground structures. We think the scripts may help readers have a clearer understanding for the paragraph above the Fig.3.

*(5) In section 4, authors just gave the numerical results, not involved the designs of pentamode acoustic cloaks and unfeelable cloaks. This sentence has been mentioned in the sections of the introduction and the conclusions.*

**Reply:**

Thanks. We acknowledge that this sentence may trigger confusion for the major focus of this paper. It is a potential application domain of the optimized orthotropic lattices but not a major focus of this paper. The main purpose of this paper is to introduce the optimization design method we have developed and then show a range of new pentamode unit cells we have not realized or discovered. We have modified the relevant statements in the revised statements.

*(6) In the numerical results, the isotropic, transverse isotropic, and orthotropic pentamode unit cells were shown. Did they use the same mathematical optimization model Eq. (17)? What are the physical meanings of the maximum eigenvalue max _1 and the second maximum eigenvalue max _2?*

**Reply:**

Yes, they use the same model originally given in Eq (17), since isotropic, transverse isotropic and orthotropic pentamode unit cells are all special cases of pentamode unit cells with at least orthotropic symmetry. For perfect pentamode metamaterials, $\lambda_{\max\_2}$ should approach zero. It is noted that $\lambda_{\max\_2}$ does not always correspond to the shear modulus, and its physical meaning is inconstant. For perfect pentamode metamaterials, $\lambda_{\max\_1}$ should be relatively large, and have the following relationship:

$$\boldsymbol{C}\boldsymbol{x} = \lambda_{\max\_1} \cdot \boldsymbol{x}$$

where $\boldsymbol{C}$ is the elasticity matrix, and $\boldsymbol{x}$ is the eigenvector corresponding to $\lambda_{\max\_1}$. It is noted that only for isotropic pentamode unit cells, then $\lambda_{\max\_1}$ is three times the bulk modulus.

*(7) The paper lacks the analysis and discussion for the optimal results. The pentamode unit cells with different relative densities are listed and prototyped. What's the purpose of authors?*

*Overall speaking, the paper needs a deep revision before publication.*

**Reply:**

Thanks for the suggestion. The analysis and discussion for the optimization results have been added in Section 4.2 and Section 4.3. Our purpose of Section 4.4 is to prove that, based on the optimized skeleton, pentamode unit cells with different relative densities can be easily obtained by just changing the geometric dimensions and shapes of the bars. This feature can be specially used in acoustic cloaking design. Finally, we show the figures of the prototyped specimens to demonstrate that the micro-lattices can be manufactured by using existing additive manufacturing techniques.

**Reviewer #2**:

This paper analyzes the necessary and sufficient boundary conditions of orthotropic pentamode materials. Two cases are considered, corresponding to zero and nonzero shear modulus. The nonzero shear modulus is set at a higher value, and the geometry design optimization is conducted to find structures of this type. The genetic-algorithm-based ground structure method is adapted to find eight isotropic pentamode structures, eight transversely isotropic pentamode structures, eight orthotropic pentamode unit cells.

*1. The literature review on page 2 is not vital, just monotonous. There is no critical discussion - e.g., the advantages and disadvantages of the previous work with reasons. For example. "Huang et al. [9] student pentamode behavior and acoustic bandgaps of diamond type pentamode lattices with various cross=sectional shape, and found that the triangle case performs best." Why?*

**Reply:**

Thanks for the suggestion. We have tried our best to revise the literature review. For the reference [9], the paper quantitatively compared numerical analysis results of different cross-section shapes and found that the triangle case performs best with lower frequency and broader bandwidth.

*2. Pentamode structures are minimal applications - mechanical cloaking. The chance of application for structural application is meager due to the fragile part. Even though it boasts a high bulk modulus, local micro buckling can quickly fail the structure.*

**Reply:**

The concept of pentamode metamaterials indeed paves a new pathway for discovering new architected composite materials and new applications. Yes, the conventional rigid-body double-cone designs with tiny and brittle tip-to-tip connections are easily subject to fracture and breakage in engineering practice. However, we would highlight that our research is exactly motivated to overcome the current bottleneck through the whole strain energy and deformation of the entire lattice architecture by topologically optimized microstructures, rather than via the highly localized tip-to-tip rigid-body deformation. At the first look, it seems that the geometrical shapes of our designs are similar to the conventional rigid-body double-cone designs. However, our designs are based on the whole elastic deformation of the entire microstructure, not the point-wide rigid-body connections. Structural strain energy-driven elastic deformation is essentially different from the ideally tip-to-tip rigid body deformation.

This is the key benefit of the topologically optimized elastic lattices, compared to conventional doble-cone rigid-body lattices. The topological designs in this paper do not have to be connected through tiny-tip connections to enable the deformation, because the uniform truss bar structures are used in our designs. However, we have involved double cone shapes into the topological designs in that the double cone shapes will conveniently benefit the change of the effective mass of the micro lattice, and therefore the application of cloaks.

*3. The conventional isotropic pentamode structures have a high bulk to shear moduli ratio. What is the mechanical feature of your orthotropic pentamode structures?*

**Reply:**

Thanks for this insightful question. For a theoretically perfect pentamode metamaterial, it can only bear one stress state, proportional to the eigenvector corresponding to the non-zero eigenvalue of its elasticity matrix [1]. This is an essential characteristic of pentamode metamaterials [1]. As a special case, isotropic pentamode can only bear a stress proportional to $[1 \quad 1 \quad 1 \quad 0 \quad 0 \quad 0]^{\mathrm{T}}$ (i.e. hydrostatic pressure). The high ratio of the bulk modulus to the shear modulus is an equivalent description only limited to the isotropic case. For transverse isotropic and orthotropic pentamode unit cells obtained in this paper, their mechanical feature is the same as their essential characteristic mentioned above. We have more detailedly explained about it right after the Eq (16).

*4. One of the biggest concerns is that there is no verification of the model - experiments and simulations should be added to the current version. Otherwise, it is hard to convince your model to work.*

**Reply:**

Thanks for the suggestion. Yes, it is indeed important to conduct experimental testing and characterization of the optimized design. However, the major focus of this paper is to the analysis and design of pentamode metamaterials with at least orthotropic symmetry. We also showcase that the optimized designs can be manufactured by using the state-of-the-art additive manufacturing techniques. A through experimental investigation is therefore beyond the major scope of this paper. However, following the reviewer's suggestion, we have added two detailed numerical simulation results of pentamode lattices using commercial software (Abaqus) in Section 4.2 and Section 4.3.

*5. It may be easier to image geometries if you add a small assembly of unit cells, e.g., two by two.*

**Reply:**

Thanks for your suggestion. We have added a $2 \times 2 \times 2$ assembly for each unit cell in Section 4.1.

*6. Please add a short description for every subfigure.*

**Reply:**

Thanks for the suggestion. We have added sub-titles for every subfigure now.

**Reviewer #3:**

The stiffness deduction of pentamode lattices structure and the optimization design of genetic algorithm are investigated in this paper. The research field is belong to the forefront of the discipline, and has a strong theoretical significance and engineering background.

*1. The stiffness deduction is the basic analysis method of pentamode lattices structure, which can not be an innovation point.*

**Reply:**

Thanks. For previous studies on the isotropic pentamode unit cell, a relatively large ratio of the bulk modulus to the shear modulus (i.e. B/G) is usually used to judge whether a unit cell is pentamode or not. However, it is not the essential and original definition of pentamode metamaterials, such as Mejica and Lantada [21] considered some non-isotropic unit cells with large B/G ratios as pentamode. Therefore, as the foundation of establishing the mathematical optimization model, we must firstly derive the necessary and sufficient condition required for elasticity constants of pentamode unit cells, instead of still using the conventional B/G ratio as the objective function.

However, we acknowledge that the purpose of the derivation is mainly for establishing the mathematical optimization model, and the derivation is important, but it cannot be considered as an independent innovation point. We have revised several statements to avoid misleading in the abstract.

*2. Genetic method was used to obtain the structure type, but the paper does not describe the establishment of the optimization model in detail. The theory in the first part can't directly deduce the objective function and constraint conditions of the optimization model, so it is suggested that the author should increase the establishment description of the optimization model.*

**Reply:**

Thanks. We have added a detailed description in Section 3.1.

*3. The author did not introduce the genetic algorithm in detail, how to calculate the number of operations?*

**Reply:**

Thanks for the suggestion. We have added a simple introduction of the genetic algorithm in Section 3.2. It is noted that we use the Matlab built-in function to implement the classical genetic algorithm, and how to develop or improve the genetic algorithm is not our major effort in this paper. This section is to emphasize that the discrete optimization problem in this paper is relatively small-scale and cheap in computation, and therefore the genetic algorithm can be used as an optimization solver, instead of mathematical programming methods that are frequently used in topology optimization.

*4. In the optimization design, the finite element model is used in the single calculation. Which responses of the structure are output to calibrate the stiffness of the structure? The article doesn't explain.*

**Reply:**

Thanks. We calculated the effective elasticity matrices of unit cells by using the typical numerical homogenization method [32], which is simply mentioned right after Eq (24). We have added a more detailed description at the beginning of Section 3.1.

*5. In this paper, several new pentamode lattices structures are presented, but the structural stiffness and structural types of new structures are not discussed. There is little discussion on the optimization model and no comparative analysis with the existing model.*

**Reply:**

We have added two sections to address the analysis and discussion of the optimization results (Section 4.2 and Section 4.3).

*6. In this paper, a typical pentamode lattices structure is established. The overall modulus is 113.8Gpa, which is equivalent to the modulus of titanium alloy, and the relative density is about 1%. What kind of material is used to print this structure? Moreover, according to the topology optimization, the shear stiffness is 0.091 and 0.42, which is far from 0 required in the model establishment. How to explain it?*

**Reply:**

Thanks for these detailed and good questions.

(1) In the finite element analyses, Ti6Al4V is chosen as the base material of unit cells. We have noted that at the end of the second paragraph in Section 4.2. The relative density 1.143% means that when the bounding box of the unit cell is $1\ \mathrm{mm} \times 1\ \mathrm{mm} \times 1\ \mathrm{mm}$, the total volume of base material in the unit cell is 0.01143 $\mathrm{mm}^3$. For the additively manufactured specimen, TangoGray FLX950 is used to print the micro-lattice, as mentioned right before Fig.18. It is noted that the material used for printing is not related to finite element analysis results from Table 1 to Table 6 at all.

(2) It is noted that perfect pentamode unit cells with zero shear moduli only exist in theory, and ideally the fluidics. In this paper, we have attempted to design solid micro lattices to approximately mimic the behavior of the fluidics. In this setting, it is not possible for the topologically optimized solid micro lattices to have the ideal properties of perfect pentamode materials. Therefore, the previous studies on numerical analyses and experiments of diamond-type isotropic pentamode unit cells all only require a relatively large ratio of the bulk modulus to the shear modulus (B/G), but not vanishing shear moduli in theory. In the Eq (24), the objective function only requires the shear moduli to be as small as possible but not to be strictly zero.

*7. The abstract cannot directly propose the purpose and conclusion of the author's research, which needs revised.*

**Reply:**

Thanks。 We have revised the abstract.

# Topological Design of Pentamode Lattice Metamaterials Using A Ground Structure Method

Zuyu Li [a], Zhen Luo [a,*], Lai-Chang Zhang [b], Chun-Hui Wang [c]

[a] School of Mechanical and Mechatronic Engineering
University of Technology Sydney, Sydney, NSW 2007, Australia
[*]Corresponding authors: zhen.luo@uts.edu.au, A/Prof Zhen Luo

[b] School of Engineering
Edith Cowan University, Perth, WA 6027, Australia

[c] School of Mechanical and Manufacturing Engineering
University of New South Wales, Sydney, NSW 2052, Australia

## Abstract

Pentamode metamaterials are a new class of artificially engineering three-dimensional lattice composites. There exist a few types of pentamode metamaterials that are dominated by ad hoc design motifs, while a systematic design approach is still missing. This paper will present an efficient topological optimization methodology to discover a series of novel pentamode lattice microarchitectures over a range of effective material properties. Firstly, the necessary and sufficient condition that is required for elasticity constants of pentamode micro lattices with at least elastically orthotropic symmetry is derived. Secondly, a general mathematical formulation for design optimization of such pentamode micro lattices is developed. Thirdly, a truss-based three-dimensional ground structure with geometrically orthotropic symmetry is generated, with geometric constraints to avoid intersection and overlap of truss bars within the ground structure. The genetic algorithm is then used to solve the topology optimization problem described by the ground structure. Finally, twenty-four pentamode lattices are designed to demonstrate the effectiveness of the proposed method.

*Keywords*: Pentamode metamaterials; Micro lattice; Orthotropic symmetry; Topology optimization; Ground structure method

## 1. Introduction

Pentamode metamaterials belong to a kind of three-dimensional solid mechanical metamaterials that are artificially architected to only bear single mode of stress [1]. A pentamode metamaterial only has one non-zero eigenvalue from its sixth-order elasticity matrix, and therefore it can deform easily in five independent modes corresponding to five zero eigenvalues from its elasticity matrix [1, 2]. Take an isotropic pentamode metamaterial as an example, it has a finite bulk modulus but a vanishing shear modulus and can only bear hydrostatic stress. In other words, they are three-dimensional lattice microstructures engineered to mimic the behavior of fluids. The unusual mechanical properties of pentamode metamaterials are gained from the geometries of their rationally designed microarchitectures, rather than the chemical compositions of their base materials (e.g., metals and polymers).

The pentamode metamaterial was first designed by Milton and Cherkaev in 1995 [1]. They are dominantly featured with a diamond-type lattice, consisting of four double-cone rigid-body bars that are jointed only at their point-like tips [1]. However, lattice microarchitectures with such point-like tips cannot stably exist in real-world applications. The infinitely small joints were therefore given finite cross-sections to facilitate manufacturing of the pentamode lattices in practice [3]. This conventional diamond-type pentamode lattice [3] is illustrated in Fig.1a, having a smaller diameter $d$ at the joints, a relatively large diameter $D$ at the midspan and a total length $l$ of a double-cone bar as shown in Fig.1b. For the double-cone lattice, the work [4] showed that using asymmetric double-cone bars can increase the ratio of the bulk modulus to the shear modulus. Huang et al. [5] quantitatively compared the pentamode behavior and acoustic bandgaps of the diamond-type pentamode lattices with five different cross-sectional shapes, and found that the triangle case performs best with lower frequency and broader bandwidth than other four shapes.

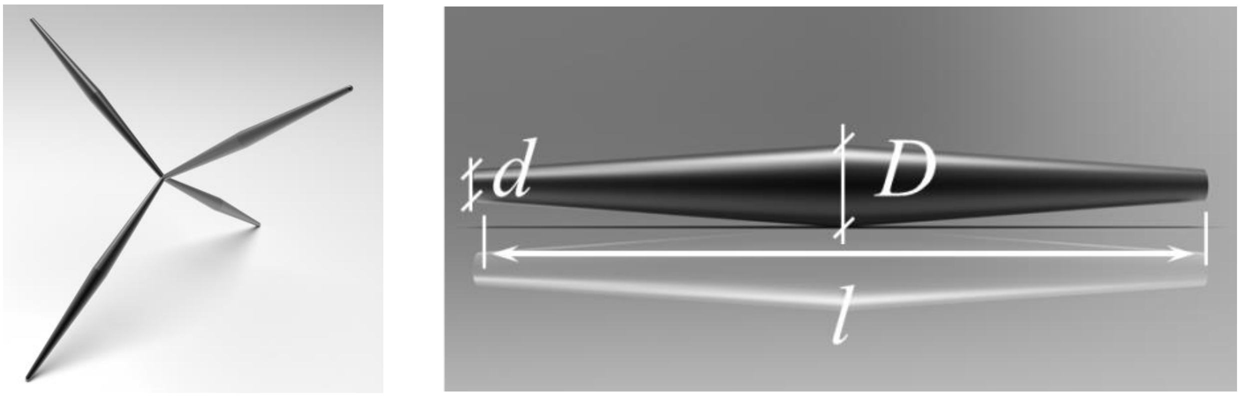


(a) Diamond-type lattice (b) Double-cone bar

**Fig.1.** Diamond-type pentamode lattice with double-cone bars

Isotropic pentamode metamaterials can uncouple the compression wave and shear wave, as ideally the bulk moduli can be infinitely large compared to the shear moduli [3]. In other words, they are difficult to compress while easily flow away, for which they are also named as metafluids [6]. Kadic et al. [3] should be the first group implemented the diamond-type pentamode lattice using dip-in direct-laser-writing optical lithography. The testing results of the manufactured diamond-type metal pentamode lattices revealed that the shear and Young's moduli are in good agreement with their theoretical calculations [7], and the elastic modulus and yield stress were decoupled from the relative density [8].

Pentamode metamaterials are promising for transforming elastostatics and particularly elastodynamics to enable acoustic cloaks [9-15], based on the concept of transformation optics but beyond that. In 2008, Norris [9] investigated the transformation acoustic cloaks and noted that ideal acoustic cloaks can be achieved through pentamode metamaterials. Compared with conventional inertial cloaks, pentamode acoustic cloaks can avoid mass singularity and be engineered with pure solid materials and are theoretically broadband since they invoke only quasi-static stiffness of pentamode metamaterials [12]. Potential applications of pentamode metamaterials in other fields have also been studied recently. For instance, Buckmann et al. [16] designed an elasto-mechanical unfeelability cloak using the conventional diamond-type pentamode metamaterials to hide hard objects and make them unfeelable. Hai et al. [17] used bimodal structures to design two-dimensional unfeelable mechanical cloaks to reduce the influence of a hole in the structure on stress concentrations and redistribute the strain. Fabbrocino et al. [18] proposed a tunable seismic base-isolation device by the combination of pentamode lattices and tensegrity structures.

It is noted that several 'pentamode metamaterials' given in literatures [11-14] are actually two-dimensional bimode metamaterials. Strictly speaking, they should have not been classified as pentamode metamaterials because three-dimension with sixth-order elasticity matrices is a necessity to define the term of penta referring to five. Of cause, a pentamode metamaterial can be considered as a three-dimensional extension of a two-dimensional bimode honeycomb metamaterial that has three linkages meet at a point. Therefore, Morse and Cherkaev [1] noted that a natural candidate might have four linkages meet at a point, which helped to discover the diamond-type pentamode lattices. Inspired by the concept of the Bravais lattices, Mejica and Lantada [19] presented a library of lattices claimed to be pentamode in 2013, but Xu [20] stated that although these lattices are not pentamode although have large ratios of the bulk modulus to the shear modulus. This phenomenon will be explained in Section 2 of this paper. In 2015, Xu [20] presented five pentamode lattices that all have only one non-zero eigenvalue from the effective elasticity matrix. In 2019, Li and Vipperman [21], and Huang et al. [22] further proposed two isotropic pentamode lattices. From the above, we can find that seven new pentamode lattices have been found but through ad hoc and empirical design methods since 1995. A generative design optimization approach that can systematically discover a range of novel pentamode lattices over a wide scope of effective properties is still missing.

Milton and Cherkaev [1] noted that pentamode metamaterials can be anisotropic. However, this possibility was not addressed and come into reality until 2013, when Kadic et al. [23] introduced intentional anisotropy into the conventional diamond-type lattices by moving just one connection point along the space diagonal. As mentioned by Milton et al. [24], pentamode metamaterials should be able to bear any chosen stress, not only isotropic. Anisotropic pentamode metamaterials are the prerequisite for realizing many applications including acoustic clocks based on transformation elastodynamics [23]. Hence, this work will focus on topology optimization of more general pentamode metamaterials not limited to isotropic. An evolutionary ground structure method using the genetic algorithm is proposed to discover novel pentamode lattice microstructures with at least orthotropic symmetry.

## 2. Necessary and sufficient condition

This section will rigorously derive the necessary and sufficient condition required for elasticity matrices of pentamode metamaterials with at least orthotropic symmetry. It is noted that the derivation here is valid for linear elasticity. For three-dimensional elasticity problem, Hooke's law is here considered in the form $\boldsymbol{\sigma} = \boldsymbol{C}\boldsymbol{\varepsilon}$, where $\boldsymbol{\sigma}$ is the vector of stress, and $\boldsymbol{\varepsilon}$ is the vector of strain. For any elastic material with orthotropic symmetry, the elasticity matrix $\boldsymbol{C}$ is defined in Eq (1). It is noted that an elasticity matrix is always positive semidefinite, i.e., $C_{ii} \geq 0$ $(i = 1,2,3,4,5,6)$.

$$\boldsymbol{C} = \begin{bmatrix} C_{11} & C_{12} & C_{13} & 0 & 0 & 0 \\ & C_{22} & C_{23} & 0 & 0 & 0 \\ & & C_{33} & 0 & 0 & 0 \\ & & & C_{44} & 0 & 0 \\ & & & & C_{55} & 0 \\ & & & & & C_{66} \end{bmatrix} \tag{1}$$

The essential definition of a pentamode metamaterial is that it has only one non-zero eigenvalue from its sixth-order elasticity matrix [1, 9]. The characteristic polynomial of the elasticity matrix in Eq (1) can be defined as:

$$|\boldsymbol{C} - \lambda \boldsymbol{I}| = (C_{44} - \lambda)(C_{55} - \lambda)(C_{66} - \lambda)(A_1 + (A_2 + (A_3 - \lambda)\lambda)\lambda) = 0 \tag{2}$$

where

$$\begin{cases} A_1 = C_{11}C_{22}C_{33} + 2C_{12}C_{13}C_{23} - C_{11}{C_{23}}^2 - C_{22}{C_{13}}^2 - C_{33}{C_{12}}^2 \\ A_2 = {C_{12}}^2 - C_{11}C_{22} + {C_{13}}^2 - C_{11}C_{33} + {C_{23}}^2 - C_{22}C_{33} \\ A_3 = C_{11} + C_{22} + C_{33} \end{cases} \tag{3}$$

To find the necessary and sufficient condition for this characteristic polynomial to have only one non-zero root, we should consider through two different cases.

The first case is that at least one of $C_{44}$, $C_{55}$ and $C_{66}$ is positive, e.g., $C_{44} > 0$. If so, the only non-zero eigenvalue should be $\lambda = C_{44}$, and then the following conditions must be satisfied:

$$\begin{cases} C_{55} = C_{66} = 0 \\ A_1 = A_2 = A_3 = 0 \end{cases} \tag{4}$$

Since the elasticity matrix is positive semidefinite, the second equation in Eq (4) equals to the following condition:

$$C_{11} = C_{22} = C_{33} = C_{12} = C_{13} = C_{23} = 0 \tag{5}$$

The derivation for $C_{55} > 0$ or $C_{66} > 0$ is the same. Therefore, the general necessary and sufficient condition for this first case is that only one of $C_{44}$, $C_{55}$ and $C_{66}$ is positive while all other elastic constants are zero, which corresponds to a lattice that can only bear one shear stress mode, which is well in line with the definition of pentamode materials in [1].

It is noted that in this paper we will only consider the second case described below for design optimization since it is more complicated and physically meaningful. The second case is that at least one of $C_{11}$, $C_{22}$ and $C_{33}$ is positive. If so, the only non-zero eigenvalue should be $\lambda = A_3 = C_{11} + C_{22} + C_{33}$, and then the following conditions must be satisfied:

$$\begin{cases} C_{44} = C_{55} = C_{66} = 0 \\ A_1 = A_2 = 0 \end{cases} \tag{6}$$

For the equation $A_1 = 0$ in Eq (6) to have three real roots as $C_{12}, C_{13}$ and $C_{23}$, from mathematical knowledge we can know that the following conditions must be satisfied:

$$\begin{cases} 4{C_{13}}^2{C_{23}}^2 - 4C_{33}\left(C_{11}{C_{23}}^2 + C_{22}{C_{13}}^2 - C_{11}C_{22}C_{33}\right) \geq 0 \\ 4{C_{12}}^2{C_{23}}^2 - 4C_{22}\left(C_{11}{C_{23}}^2 + C_{33}{C_{12}}^2 - C_{11}C_{22}C_{33}\right) \geq 0 \\ 4{C_{12}}^2{C_{13}}^2 - 4C_{11}\left(C_{22}{C_{13}}^2 + C_{33}{C_{12}}^2 - C_{11}C_{22}C_{33}\right) \geq 0 \end{cases} \tag{7}$$

which can be simplified as:

$$\begin{cases} \left({C_{13}}^2 - C_{11}C_{33}\right)\left({C_{23}}^2 - C_{22}C_{33}\right) \geq 0 \\ \left({C_{12}}^2 - C_{11}C_{22}\right)\left({C_{23}}^2 - C_{22}C_{33}\right) \geq 0 \\ \left({C_{12}}^2 - C_{11}C_{22}\right)\left({C_{13}}^2 - C_{11}C_{33}\right) \geq 0 \end{cases} \tag{8}$$

These inequality equations require the values of ${C_{12}}^2 - C_{11}C_{22}$, ${C_{13}}^2 - C_{11}C_{33}$ and ${C_{23}}^2 - C_{22}C_{33}$ to have no opposite signs. Combined with the equation $A_2 = 0$ in Eq (6), we can know that the following condition must be satisfied:

$${C_{12}}^2 - C_{11}C_{22} = {C_{13}}^2 - C_{11}C_{33} = {C_{23}}^2 - C_{22}C_{33} = 0 \tag{9}$$

which can be simplified to be:

$$\begin{cases} C_{12} = a\sqrt{C_{11}C_{22}} \\ C_{13} = b\sqrt{C_{11}C_{33}} \\ C_{23} = c\sqrt{C_{22}C_{33}} \end{cases} \tag{10}$$

where

$$a = \pm 1, \qquad b = \pm 1, \qquad c = \pm 1 \tag{11}$$

Moreover, from the equation $A_1 = 0$ in Eq (6), we can know that:

$$C_{11}C_{22}C_{33} + 2C_{12}C_{13}C_{23} = (1 + 2abc)C_{11}C_{22}C_{33} = C_{11}{C_{23}}^2 + C_{22}{C_{13}}^2 + C_{33}{C_{12}}^2 \geq 0 \tag{12}$$

This inequality equation additionally requires that:

$$abc \neq -1 \tag{13}$$

Eq (11) and Eq (13) can be combined to meet the following four cases:

$$\begin{cases} a = b = c = 1 & \text{or} \\ a = 1, b = c = -1 & \text{or} \\ b = 1, a = c = -1 & \text{or} \\ c = 1, a = b = -1 \end{cases} \tag{14}$$

It is noted that the condition above also contain the case that only one or two of $C_{11}$, $C_{22}$ and $C_{33}$ is positive while all other elastic constants are zero. Therefore, the necessary and sufficient condition required for elastic materials with at least orthotropic symmetry to be pentamode for the second case is the combination of Eq (10), Eq (14) and the equation $C_{44} = C_{55} = C_{66} = 0$ in Eq (6). When satisfying this necessary and sufficient condition, the elasticity matrix can be simplified as:

$$
\boldsymbol{C} = \begin{bmatrix} C_{11} & a\sqrt{C_{11}C_{22}} & b\sqrt{C_{11}C_{33}} & 0 & 0 & 0 \\ & C_{22} & c\sqrt{C_{22}C_{33}} & 0 & 0 & 0 \\ & & C_{33} & 0 & 0 & 0 \\ & & & 0 & 0 & 0 \\ & & & & 0 & 0 \\ & & & & & 0 \end{bmatrix} \tag{15}
$$

The corresponding eigenvector of the only one non-zero eigenvalue $\lambda = C_{11} + C_{22} + C_{33}$ is:

$$
\boldsymbol{x} = \begin{bmatrix} ab\sqrt{C_{11}} & ac\sqrt{C_{22}} & bc\sqrt{C_{33}} & 0 & 0 & 0 \end{bmatrix}^{\mathrm{T}} \tag{16}
$$

As mentioned above, a pentamode metamaterial has only one non-zero eigenvalue from its sixth-order elasticity matrix [1, 9]. It indicates that there are five independent strain cases that each strain case or their linear combinations will produce zero stress and zero strain energy [6]. It also indicates that this kind of materials can only bear single mode of stress, corresponding to the non-zero eigenvalue [1]. As a special case, isotropic pentamode metamaterials must have the following type of elasticity matrix:

$$
\boldsymbol{C} = \begin{bmatrix} C_{11} & C_{11} & C_{11} & 0 & 0 & 0 \\ \blacksquare & C_{11} & C_{11} & 0 & 0 & 0 \\ \blacksquare & \blacksquare & C_{11} & 0 & 0 & 0 \\ \blacksquare & \blacksquare & \blacksquare & 0 & 0 & 0 \\ \blacksquare & \blacksquare & \blacksquare & \blacksquare & 0 & 0 \\ \blacksquare & \blacksquare & \blacksquare & \blacksquare & \blacksquare & 0 \end{bmatrix} \tag{17}
$$

For the above elasticity matrix, there is only one non-zero eigenvalue $\lambda = 3C_{11}$, and its corresponding eigenvector is $[1 \quad 1 \quad 1 \quad 0 \quad 0 \quad 0]^{\mathrm{T}}$. We can find that this non-zero eigenvalue is exactly three times the bulk modulus $B = C_{11}$, and the eigenvector indicates that the material can only bear the hydrostatic stress. Therefore, isotropic pentamode metamaterials are equivalently identified by a finite bulk modulus and a vanishing shear modulus [3, 7]. However, it is not applicable to non-isotropic pentamode metamaterials. For pentamode metamaterials with at least orthotropic symmetry, we can find that the non-zero eigenvalue $\lambda = C_{11} + C_{22} + C_{33}$ is not always proportional to its bulk modulus in Eq (18), and the eigenvector in Eq (16) does not always correspond to hydrostatic stress either.

$$
B = \frac{C_{11}C_{23}{}^2 + C_{22}C_{13}{}^2 + C_{33}C_{12}{}^2 - 2C_{12}C_{13}C_{23} - C_{11}C_{22}C_{33}}{C_{12}{}^2 + C_{13}{}^2 + C_{23}{}^2 + 2(C_{11}C_{23} + C_{22}C_{13} + C_{33}C_{12} - C_{12}C_{13} - C_{12}C_{23} - C_{13}C_{23}) - (C_{11}C_{22} + C_{11}C_{33} + C_{22}C_{33})} \tag{18}
$$

Therefore, a relatively very large ratio of the bulk modulus to the shear modulus is no more a sufficient condition for non-isotropic pentamode metamaterials. In other words, such a ratio cannot be used to identify whether an orthotropic or transverse isotropic lattice is a pentamode or not. In Mejica and Lantada [19], for example, although the lattices have large ratios of the bulk modulus to the shear modulus, they are not isotropic and their elasticity matrices have more than one non-zero eigenvalues [20].

## 3. Genetic-algorithm-based ground structure method

In this section, we propose a topology optimization method to discover novel pentamode lattices with at least orthotropic symmetry. Topology optimization is a powerful design tool able to find novel structures and materials. It is essentially a numerical process to iteratively re-distribute materials within a design domain to find the best distribution with optimized objective performance subject to a set of prescribed constraints. Topology optimization methods of continuum structures, e.g. density-based method, level set method and evolutionary structural optimization method, have been applied to design metamaterials [25-28]. For discrete structures, the most popular topology optimization method should be the ground structure method, which has also been applied in design optimization of mechanical metamaterials [29-31].

Since potential pentamode lattices to be designed in this paper have nearly zero effective shear moduli, it is expected that these lattices should behave like mechanisms and consist of hinge-type joints. However, it is difficult to obtain an optimized design with hinge joints when topology optimization methods of continuum structures with the solid finite elements are used. Hence, we will propose a ground structure method for design of pentamode metamaterials, using truss elements in the numerical homogenization of lattices.

### *3.1. Optimization formulation*

We assume that there is a truss structure with a fixed number of bars, termed as the ground structure. The active bars in the ground structure are chosen as design variables. The finally designed lattice is then formed by active bars. Using the finite element method and the numerical homogenization method, the effective elasticity matrix $\boldsymbol{C}^H$ of the lattice can be calculated by:

$$\boldsymbol{C}^H = \frac{1}{V}\boldsymbol{U}^T\boldsymbol{K}\boldsymbol{U} \tag{19}$$

where $V$ is the volume of the lattice, $\boldsymbol{K}$ is the global stiffness matrix of the structure. The displacement fields $\boldsymbol{U}$ in six load cases are calculated with the following periodic boundary condition. For every two points $p$ and $q$ that are periodically coincident on the lattice's boundaries, their nodal displacements $\boldsymbol{u}$ must satisfy the following equation:

$$\boldsymbol{u}(\boldsymbol{x}_p) - \boldsymbol{u}(\boldsymbol{x}_q) = \boldsymbol{\varepsilon}_i^0(\boldsymbol{x}_p - \boldsymbol{x}_q) \tag{20}$$

where $\boldsymbol{x}$ is the point coordinate, and $\boldsymbol{\varepsilon}_i^0$ is the prescribed macroscopic strain of the i-th load case. For each load case, only one strain component is set to unit whereas the rest five as zero. In other words, the prescribed macroscopic strains for the six load cases are $\boldsymbol{\varepsilon}^0 = \boldsymbol{I}$. To prevent rigid body motions, displacements of one arbitrary point should be fixed. For theoretical and numerical implantation details of the typical numerical homogenization method, readers may refer to [32].

After obtaining the homogenized effective elasticity matrix, we should establish a fitness function to justify whether it satisfies the necessary and sufficient condition derived in Section 2 for pentamode metamaterials with at least orthotropic symmetry. Firstly, for metamaterials with at least orthotropic symmetry, it is obvious that the tension-shear coupling terms in the elasticity matrix must be zero. We exclude that these terms from the objective function and treat them as equality constraints in the mathematical model, because they can be strictly satisfied by guaranteeing that the ground structure has the geometrically orthotropic symmetry. Secondly, we rewrite the Eq (10) as the following form:

$$\frac{a\sqrt{C_{11}C_{22}}}{C_{12}} - 1 = \frac{b\sqrt{C_{11}C_{33}}}{C_{13}} - 1 = \frac{c\sqrt{C_{22}C_{33}}}{C_{23}} - 1 = 0 \tag{21}$$

which can be further simplified as:

$$\left(\frac{a\sqrt{C_{11}C_{22}}}{C_{12}}-1\right)^2+\left(\frac{b\sqrt{C_{11}C_{33}}}{C_{13}}-1\right)^2+\left(\frac{c\sqrt{C_{22}C_{33}}}{C_{23}}-1\right)^2=0 \tag{22}$$

Finally, since $C_{ii} \geq 0$ $(i = 1,2,3,4,5,6)$, we can rewrite the equation $C_{44} = C_{55} = C_{66} = 0$ in the Eq (6) as the following form:

$$\frac{C_{44}+C_{55}+C_{66}}{C_{11}+C_{22}+C_{33}}=0 \tag{23}$$

Therefore, the sum of left-side terms in Eq (22) and Eq (23) must also be zero. Then a general mathematical optimization model can be defined as follows:

Find: $\boldsymbol{\rho} = [\rho_1 \quad \rho_2 \quad \cdots \quad \rho_{n_{bar}-1} \quad \rho_{n_{bar}}]$

$$\begin{aligned}\text{Min:}\, f(\boldsymbol{\rho}) = &\left(\frac{a\sqrt{C_{11}{}^H(\boldsymbol{\rho})C_{22}{}^H(\boldsymbol{\rho})}}{C_{12}{}^H(\boldsymbol{\rho})}-1\right)^2+\left(\frac{b\sqrt{C_{11}{}^H(\boldsymbol{\rho})C_{33}{}^H(\boldsymbol{\rho})}}{C_{13}{}^H(\boldsymbol{\rho})}-1\right)^2+\left(\frac{c\sqrt{C_{22}{}^H(\boldsymbol{\rho})C_{33}{}^H(\boldsymbol{\rho})}}{C_{23}{}^H(\boldsymbol{\rho})}-1\right)^2 \\ &+\frac{C_{44}{}^H(\boldsymbol{\rho})+C_{55}{}^H(\boldsymbol{\rho})+C_{66}{}^H(\boldsymbol{\rho})}{C_{11}{}^H(\boldsymbol{\rho})+C_{22}{}^H(\boldsymbol{\rho})+C_{33}{}^H(\boldsymbol{\rho})}\end{aligned} \tag{24}$$

$$\text{S.t.}\ \begin{cases} C_{ij}{}^H(\boldsymbol{\rho}) = 0, \quad i = 1,2,3 \quad j = 4,5,6 \\ C_{45}{}^H(\boldsymbol{\rho}) = C_{46}{}^H(\boldsymbol{\rho}) = C_{56}{}^H(\boldsymbol{\rho}) = 0 \end{cases}$$

where $\boldsymbol{C}^H$ is the effective elasticity matrix of the ground structure estimated by the numerical homogenization method considering the periodic boundary condition [32], $\boldsymbol{\rho}$ is a vector of binary variables representing whether each bar in the ground structure is active or not, $n_{bar}$ is the number of bars in the ground structure. It is noted that a choice of $a$, $b$ and $c$ that belongs to the four cases in Eq (14) should be determined in advance. We would emphasize that the dominator $C_{11}{}^H(\boldsymbol{\rho})+C_{22}{}^H(\boldsymbol{\rho})+C_{33}{}^H(\boldsymbol{\rho})$ is not necessary in the objective function but it is used to normalize the last term to enhance the optimization performance.

The constraints in Eq (24) are to ensure that the optimized lattices have at least orthotropic symmetry. When the objective function value approaches to zero (globally minimum value), the necessary and sufficient condition required for elasticity matrix of pentamode metamaterials with at least orthotropic symmetry will be satisfied. It is noted that for such an inverse design problem, multiple solutions may exist.

As mentioned above, the design variables are 0 and 1 logical variables representing which bars are active. However, it does not mean that inactive bars are not included in finite element analyses of the numerical homogenization. That is because the total stiffness matrix of a mechanism-type pentamode lattice that only consists of active bars is singular in numerical. Therefore, inactive bars are assigned with relatively small axial stiffness and then included in the numerical homogenization. This can prevent the total stiffness matrix from being singular but the effect to the value of the effective elasticity matrix is small and acceptable.

### *3.2. Optimization solver*

Recently, Wang et al. [31] has studied the design of materials with prescribed nonlinear properties using the ground structure method, which uses artificial densities of each bar as continuous design variables and the mathematical programming method to solve the problem. In this paper, we will also use the ground structure method to design pentamode metamaterials, but the genetic algorithm [33] is adopted to solve this discrete optimization problem with binary variables. The genetic algorithm is in general known as a global optimization method based on natural selection. It randomly generates an initial population. During the iteration, individuals with better fitness values in the current population will be selected as parents. Then three types of children are produced from parents to form the next generation. Elite children are individuals with best fitness values, crossover children are generated by combining pairs of parents, and mutation children are generated by making random changes to individual parents [33]. In the numerical implementation, we use the built-in Matlab function for the genetic algorithm.

The genetic algorithm is not often used to solve topology optimization problems for no matter continuum or discrete structures, although it is a heuristic optimization method with global searching capbility. The first main reason is that there are usually thousands or even millions of continuous design variables in topology optimization problems. It is difficult for genetic algorithms to find a solution for large-scale optimization problems with continuous variables. The second reason is that the calculation of the objective and constraint functions with large-scale finite elements is computationally expensive. Unfortunately, thousands of times of evaluation of candidate solutions is common for the genetic algorithm, while mathematical programming methods using sensitivity information usually need up to hundreds of times of finite element analyses. However, the ground structure used in this paper is a very small-scale truss model with only hundreds of binary design variables. It is also cheap in computation to run finite element analyses in parallel. Therefore, instead of using mathematical programming methods, the genetic algorithm is used in this paper as the optimization solver to find the global optimal solution, since the discrete optimization problem here is relatively small scale and cheap in computation.

In this work, the max number of optimization iterations is set to 200, and the population size is 1000. Calculation of the objective function runs in parallel using a 6-core Intel i7-8750H CPU. For the maximum 0.2 million times of finite element analyses and numerical homogenization evaluations, it only costs around 25 minutes when using the ground structure described in Section 3.3.

### *3.3. Generation of the ground structure*

For a given set of mesh nodes, the easiest way to generate a ground structure is just linking every two nodes. The number of bars for such a fully connected ground structure is equal to $({n_{node}}^2 - n_{node})/2$, where $n_{node}$ is the number of nodes. Zegard and Paulino [34] proposed a method to generate ground structures in arbitrary three-dimensional domains with control in the level of redundancy or inter-connectedness of ground structures. However, it cannot guarantee that optimized lattices have at least orthotropic material symmetry. Therefore, a new ground structure with geometrically orthotropic symmetry is proposed in this paper to ensure that the optimized lattices always have at least elastically orthotropic symmetry. Then the constraints in Eq (24) can be automatically satisfied.

We suppose there are $5 \times 5 \times 5$ Cartesian mesh nodes centered at the origin and aligned with coordinate axes as shown in Fig.2a, and then the corresponding ground structure with geometrically orthotropic symmetry will be as shown in Fig.2b. Due to the geometrically orthotropic symmetry, the design variables are changed from $\boldsymbol{\rho}$ to $\tilde{\boldsymbol{\rho}}$ as defined in Eq (20), which is still a vector of binary design variables.

$$\tilde{\boldsymbol{\rho}} = [\tilde{\rho}_1 \quad \tilde{\rho}_2 \quad \cdots \quad \tilde{\rho}_{n_{des}-1} \quad \tilde{\rho}_{n_{des}}] \tag{25}$$

where $n_{des}$ is the number of design variables. For the ground structure in Fig. 2b, the numbers of bars and design variables are 2544 and 405 respectively, while for a fully connected ground structure both the bar number and design variables will be as large as 7750.

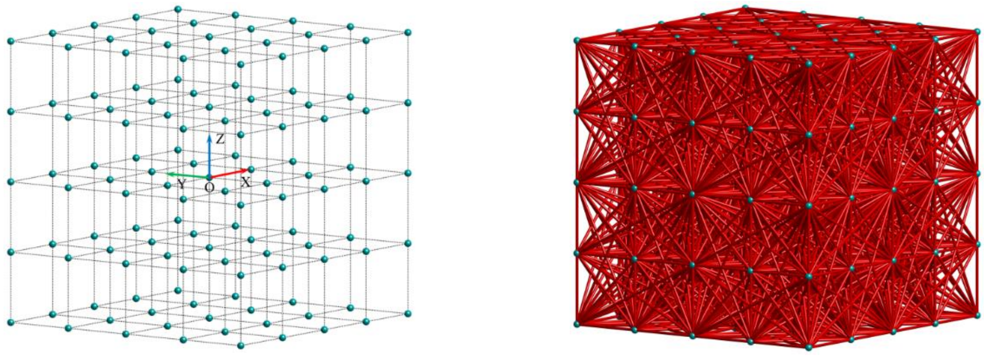


(a) Cartesian mesh nodes (b) Ground structure

**Fig.2.** Mesh nodes and the corresponding ground structure

The bars in the ground structure are divided into five groups as shown in Fig.3. The bars of the first group are collinear with one coordinate axis and symmetric about one coordinate plane. Each of these bars has no mirrored copies in the ground structure as shown in Fig.3a. Therefore, 6 design variables of this group correspond to 6 bars. The second group consists of two types of bars. One type is collinear with one coordinate axis and on the side of one coordinate plane. The other type is coplanar with one coordinate plane, parallel but not collinear with one coordinate axis and then symmetric about another coordinate plane. Each of these bars has another mirrored copy in the ground structure as shown in Fig.3b. Therefore, 33 design variables of this group correspond to 66 bars. The bars of the third group are coplanar with one coordinate plane and on the side of other coordinate planes. Each of these bars has other three mirrored copies in the ground structure as shown in Fig.3c. Therefore, 90 design variables of this group correspond to 360 bars. The bars of the fourth group are symmetric about one coordinate plane and parallel but not coplanar with other coordinate planes. Each of these bars has other three mirrored copies in the ground structure as shown in Fig.3d. Therefore, 24 design variables of this group correspond to 96 bars. Finally, the fifth group is obtained by linking every two nodes in the same octant and then subtracting bars that already belong to the aforementioned four groups. Each of these bars has other seven mirrored copies in the ground structure as shown in Fig.3e. Therefore, 252 design variables of this group correspond to 2016 bars.

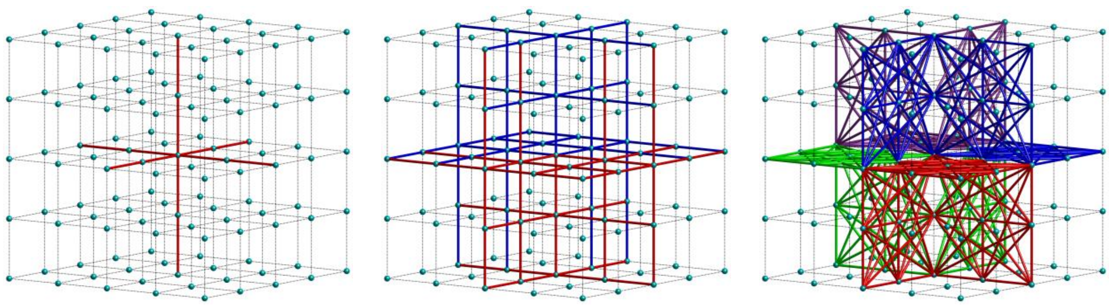

(a) Group A (b) Group B (c) Group C

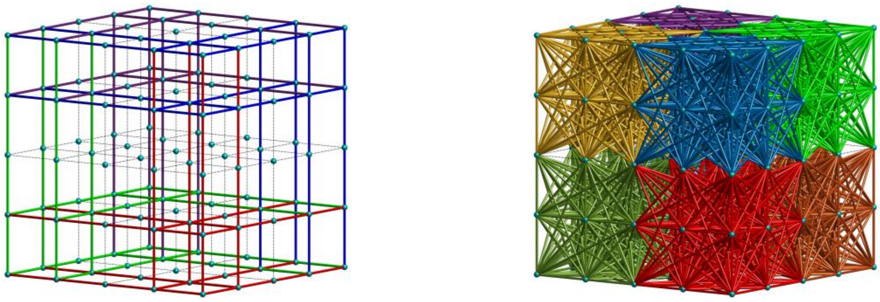

(d) Group D (e) Group E

**Fig.3.** Different groups of bars

For the educational purpose, we provide two Matlab scripts online for free download and use at https://github.com/appreciator/Ground-Structure. One script can be used to generate ground structures with geometrically orthotropic symmetry as introduced above. The other script can determine which bars are active according to the given design variables. The numbers of Cartesian mesh nodes are chosen as user-input values, and therefore the reader can obtain much more complex ground structures. It is noted that the lattices do not always have to be geometrically orthotropic symmetric. Therefore, other potential pentamode lattices without geometrically orthotropic symmetry, e.g., the conventional diamond-type pentamode lattice, cannot be discovered by using the ground structure proposed in this paper.

### *3.4. Geometric constraints*

Definitions of intersection and overlap of bars are illustrated in Fig.4.

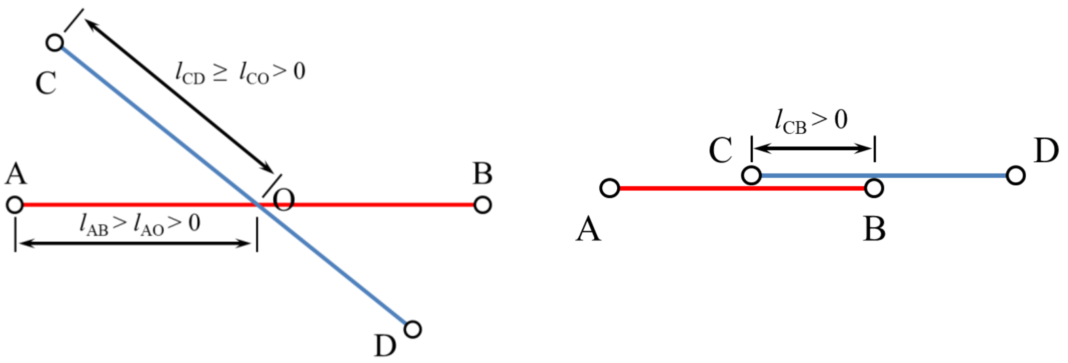


(a) Intersection (b) Overlap

**Fig.4.** Intersection and overlap of two bars

Geometric constraints on intersection and overlap of bars in ground structure methods have already been introduced for macro-scale structures [35, 36], but not yet been introduced for lattice designs [29-31]. In engineering, intersectional points have no physical meaning except in the form of hinge points [36]. Optimization solutions with existence of intersection or overlap of bars are unrealistic designs [36]. Such impractical topologies should be avoided for optimized lattices. Therefore, constraints on intersection and overlap of bars should be imposed on optimization design of pentamode metamaterials. Cui et al. [36] provided a mathematical recognition method for intersection and overlap of bars in three-dimensional ground structures. However, it is not computationally efficient, e.g. linear equations should be solved for each two bars. Based on calculating the shortest line between two lines in three dimensions, we propose a new mathematical recognition method in this paper.

As shown in Fig.5, the lines AB and CD do not intersect at a point, and the line EF is the shortest line between them. Coordinates of the points E and F are defined as:

$$\begin{cases} \boldsymbol{x}_{\mathrm{E}} = \boldsymbol{x}_{\mathrm{A}} + \mu_{\mathrm{E}}(\boldsymbol{x}_{\mathrm{B}} - \boldsymbol{x}_{\mathrm{A}}) \\ \boldsymbol{x}_{\mathrm{F}} = \boldsymbol{x}_{\mathrm{C}} + \mu_{\mathrm{F}}(\boldsymbol{x}_{\mathrm{D}} - \boldsymbol{x}_{\mathrm{C}}) \end{cases} \tag{26}$$

The values of $\mu_{\mathrm{E}}$ and $\mu_{\mathrm{F}}$ range from negative to positive infinity. $\mu_{\mathrm{E}}$ can be calculated by the following formula, while $\mu_{\mathrm{F}}$ can be calculated by substituting subscripts:

$$\mu_{\mathrm{E}} = \frac{d_{\mathrm{ACDC}} d_{\mathrm{DCBA}} - d_{\mathrm{ACBA}} d_{\mathrm{DCDC}}}{d_{\mathrm{BABA}} d_{\mathrm{DCDC}} - d_{\mathrm{DCBA}} d_{\mathrm{DCBA}}} \tag{27}$$

where

$$d_{\mathrm{MNOP}} = (x_{\mathrm{M}} - x_{\mathrm{N}})(x_{\mathrm{O}} - x_{\mathrm{P}}) + (y_{\mathrm{M}} - y_{\mathrm{N}})(y_{\mathrm{O}} - y_{\mathrm{P}}) + (z_{\mathrm{M}} - z_{\mathrm{N}})(z_{\mathrm{O}} - z_{\mathrm{P}}) \tag{28}$$

when AB and CD intersect, E and F are coincident and the values of $\mu_{\mathrm{E}}$ and $\mu_{\mathrm{F}}$ are between 0 and 1. when AB and CD are parallel, the dominator in Eq (27) is zero. Details of mathematical derivation can be referred to [37].

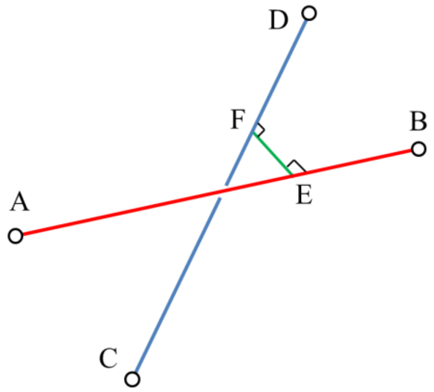


**Fig.5.** Shortest line between two lines in three dimensions

Under the assumption that AB and CD are parallel, if points A, B and C are collinear, lines AB and CD will be collinear. For three points to be collinear, the following equation should be satisfied:

$$\begin{cases} (y_{\mathrm{B}} - y_{\mathrm{A}})(z_{\mathrm{C}} - z_{\mathrm{A}}) - (y_{\mathrm{C}} - y_{\mathrm{A}})(z_{\mathrm{B}} - z_{\mathrm{A}}) = 0 \\ (x_{\mathrm{C}} - x_{\mathrm{A}})(z_{\mathrm{B}} - z_{\mathrm{A}}) - (x_{\mathrm{B}} - x_{\mathrm{A}})(z_{\mathrm{C}} - z_{\mathrm{A}}) = 0 \\ (x_{\mathrm{B}} - x_{\mathrm{A}})(y_{\mathrm{C}} - y_{\mathrm{A}}) - (x_{\mathrm{C}} - x_{\mathrm{A}})(y_{\mathrm{B}} - y_{\mathrm{A}}) = 0 \end{cases} \tag{29}$$

For two lines to be coplanar, the following equation should be satisfied:

$$\overrightarrow{\mathrm{AC}} \cdot \left(\overrightarrow{\mathrm{AB}} \times \overrightarrow{\mathrm{CD}}\right) = 0 \tag{30}$$

The flowchart about how to detect intersection and overlap of each two bars is given in Fig.6.

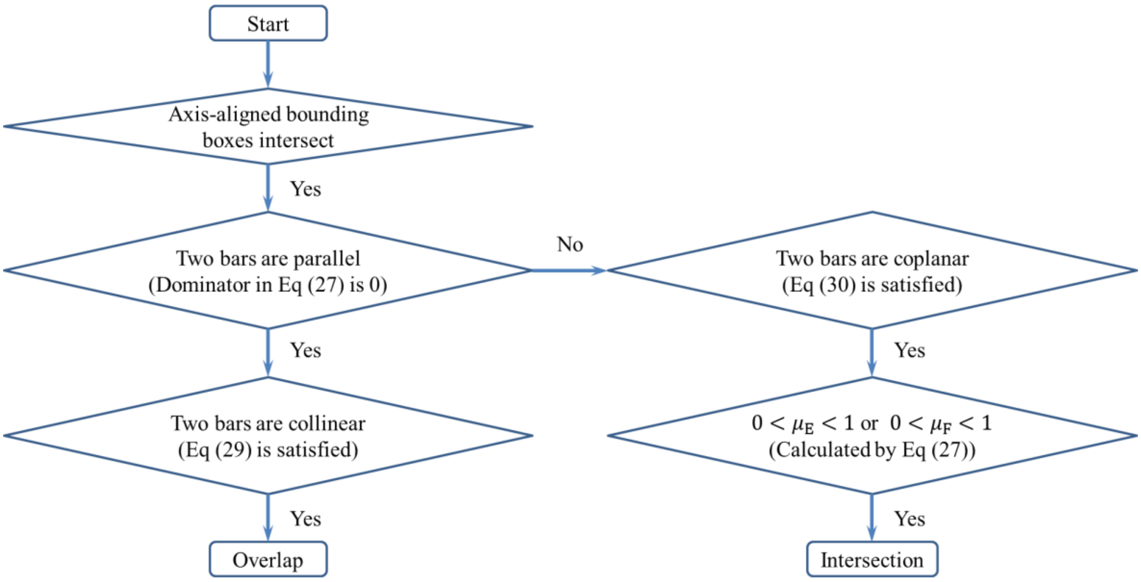


**Fig.6.** Flowchart of the detection method for intersection and overlap of bars

Since genetic algorithms cannot handle nonlinear constraints like mathematical programming methods, geometric constraints on intersection and overlap are added as a penalty term into the original objective function in Eq (24). The modified objective function is defined as:

$$\tilde{f}(\tilde{\boldsymbol{\rho}}) = f(\tilde{\boldsymbol{\rho}}) + w\frac{n_{ins}(\tilde{\boldsymbol{\rho}}) + n_{ovl}(\tilde{\boldsymbol{\rho}})}{n_{geo}} \tag{31}$$

where $n_{geo}$ is the total number of intersection and overlap of the fully active ground structure, $n_{ins}$ is the number of intersection of the current design, $n_{ovl}$ is the number of overlap of the current design, and $w$ is a weighting factor.

For a design without any intersection or overlap of bars, the penalty value becomes zero, and then the modified objective function is the same as the original one. Normalized by the dominator $n_{geo}$, the penalty value will not be larger than $w$. Since the value of $f(\tilde{\boldsymbol{\rho}})$ approaches to zero during the optimization iteration, the value of $w$ can absolutely be a small number but still relatively large enough compared with zero. Therefore, we choose $w = 0.001$ in this work.

It is noted that ground structures generated by the method in [34] do not have a single bar connecting the same nodes with other two bars as shown in Fig.7. However, these two cases of bars may have different influence on pentamode behavior of lattices, and we cannot determine which case should be adopted for different local locations in the ground structure in advance. Therefore, these two cases of bars both initially exist in the ground structure described in Section 3.3. However, we emphasize that since geometric constraints have been imposed as a penalty term in the objective function, such an overlapping case will not exist in the final optimized designs.

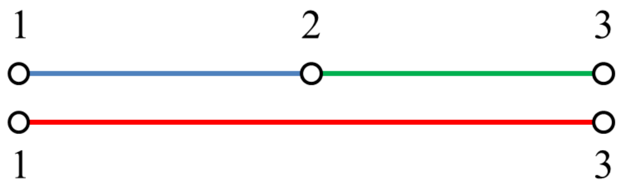


**Fig.7.** Overlapping bars in the ground structure

## 4. Numerical results

Twenty-four new pentamode lattices without any intersection or overlap of bars will be provided here to demonstrate the effectiveness of the proposed design method, including isotropic, transverse isotropic and orthotropic ones. In this section, we will give results for numerical verification of non-isotropic pentamode lattices. We will further compare the static mechanical performance of two lattices, respectively, assembled by new isotropic pentamode lattices and the conventional diamond-type isotropic lattices. Moreover, we will study on how to obtain pentamode lattices with different relative densities from the optimization results.

### *4.1. New pentamode lattices*

As shown in Fig.2b, the ground structure is generated by $5 \times 5 \times 5$ mesh nodes with 2544 bars and 405 design variables. The side length of its bounding box is 1 mm. Truss elements are used in finite element analyses. The Young's modulus is 1.138e5 MPa. Constant diameters of active and inactive bars are 0.02 mm and 2.0e-6 mm respectively. We define $\lambda_{\max\_1}$ as the maximum eigenvalue of the effective elasticity matrix of a lattice, $\lambda_{\max\_2}$ as the second maximum eigenvalue, and $\lambda_{\mathrm{R}}$ as the ratio between them. For perfect pentamode metamaterials, $\lambda_{\mathrm{R}}$ should approach infinity. In the following, three tables are given in this section, and note that the unit of elastic constants is MPa. A smaller scale of $2 \times 2 \times 2$ periodic array is given on the right side together with the lattice on the left side in each sub-figure. It is noted that each periodic array visualized here is smaller scale than the lattice.

Eight isotropic pentamode lattices are shown in Fig. 8. The corresponding effective elasticity matrices and eigenvalue ratios are listed in Table 1.

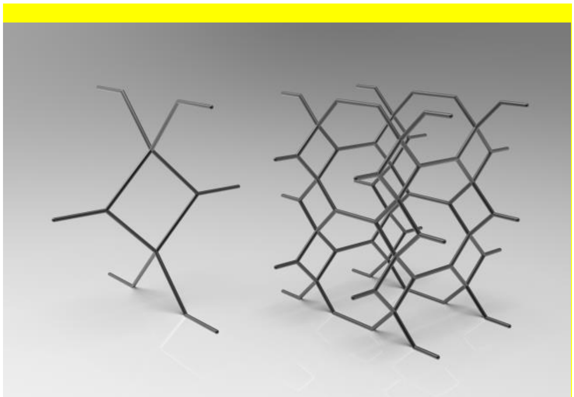

(a) Iso-a

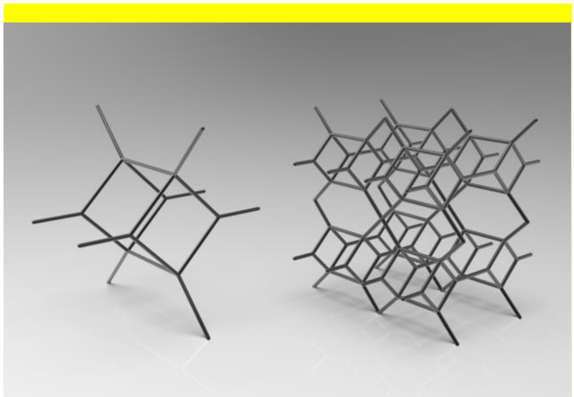

(b) Iso-b

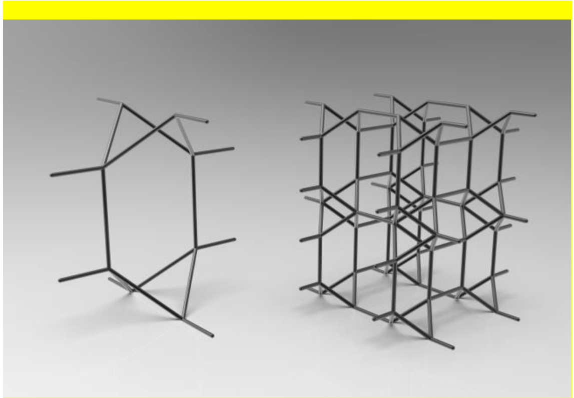

(c) Iso-c

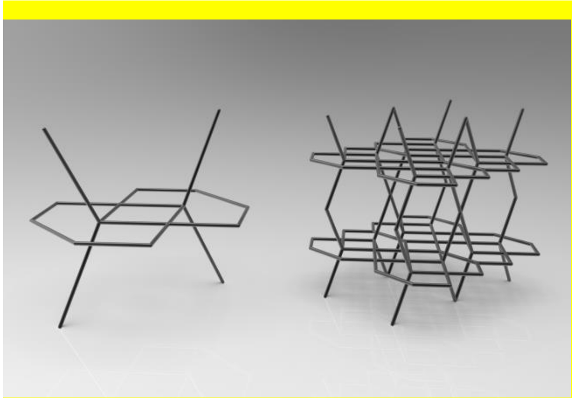

(d) Iso-d

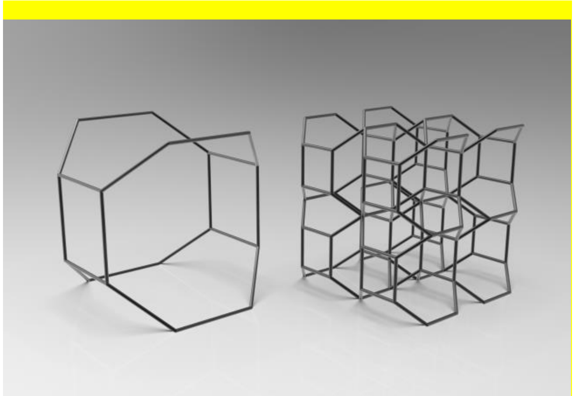

(e) Iso-e

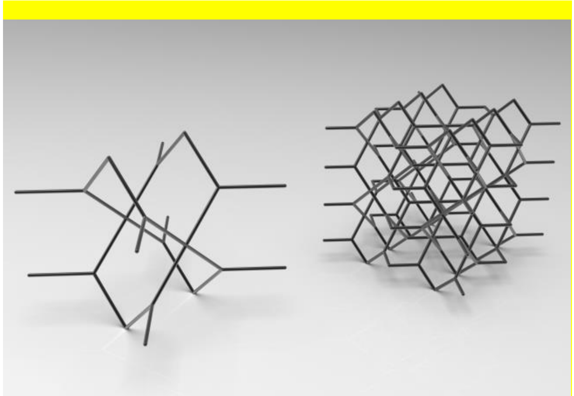

(f) Iso-f

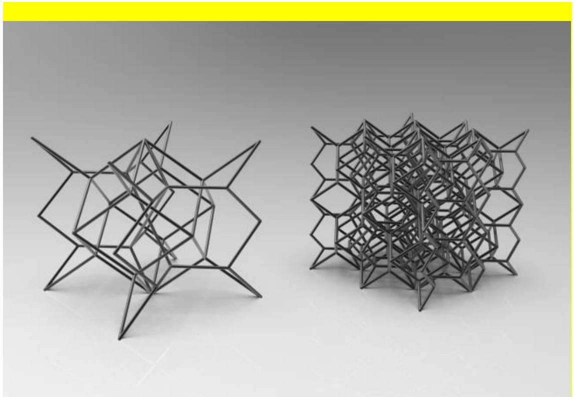

(g) Iso-g

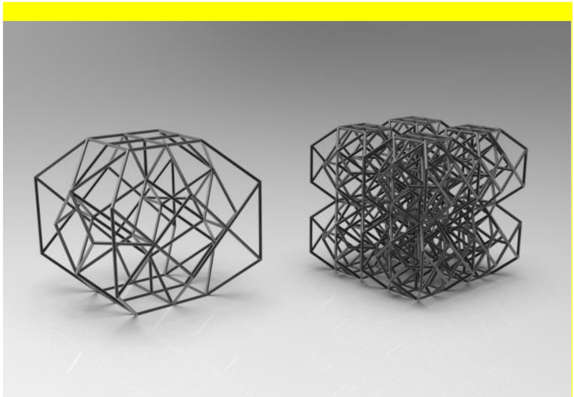

(h) Iso-h

**Fig.8.** Isotropic pentamode lattices

**Table 1.** Effective properties of isotropic pentamode lattices

| | a | b | c | d | e | f | g | h |
|---|---|---|---|---|---|---|---|---|
| $C_{11}$ | 16.519 | 22.908 | 25.546 | 27.680 | 34.896 | 33.707 | 95.491 | 125.376 |
| $C_{22}$ | 16.519 | 22.908 | 25.546 | 27.680 | 34.896 | 33.707 | 95.491 | 125.376 |
| $C_{33}$ | 16.519 | 22.908 | 25.546 | 27.680 | 34.896 | 33.707 | 95.491 | 125.376 |
| $C_{12}$ | 16.519 | 22.908 | 25.545 | 27.680 | 34.896 | 33.707 | 95.491 | 125.376 |
| $C_{13}$ | 16.519 | 22.908 | 25.545 | 27.680 | 34.896 | 33.707 | 95.491 | 125.376 |
| $C_{23}$ | 16.519 | 22.908 | 25.545 | 27.680 | 34.896 | 33.707 | 95.491 | 125.376 |
| $C_{44}$ | 3.16e-5 | 3.20e-5 | 3.19e-5 | 3.03e-5 | 3.22e-5 | 3.35e-5 | 3.79e-5 | 6.10e-5 |
| $C_{55}$ | 3.16e-5 | 3.24e-5 | 3.19e-5 | 3.29e-5 | 3.20e-5 | 3.35e-5 | 3.89e-5 | 5.90e-5 |

| | | | | | | | | |
|---|---|---|---|---|---|---|---|---|
| $C_{66}$ | 3.03e-5 | 3.03e-5 | 3.22e-5 | 4.27e-5 | 3.22e-5 | 3.35e-5 | 3.77e-5 | 4.19e-5 |
| $\lambda_{\max\_1}$ | 49.558 | 68.724 | 76.636 | 83.040 | 104.687 | 101.120 | 286.472 | 376.127 |
| $\lambda_{\max\_2}$ | 6.90e-5 | 7.19e-5 | 6.70e-5 | 8.87e-5 | 6.69e-5 | 6.61e-5 | 6.78e-5 | 8.09e-5 |
| $\lambda_{\mathrm{R}}$ | 7.18e5 | 9.55e5 | 1.14e6 | 9.36e5 | 1.56e6 | 1.53e6 | 4.22e6 | 4.65e6 |

Eight transverse isotropic pentamode lattices are shown in Fig.9. The corresponding effective elasticity matrices and eigenvalue ratios are listed in Table 2.

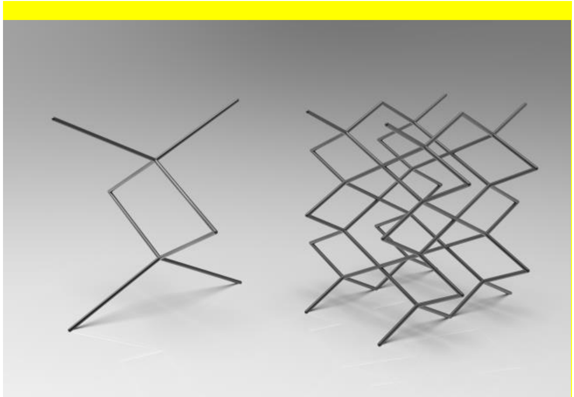

(a) Trans-a

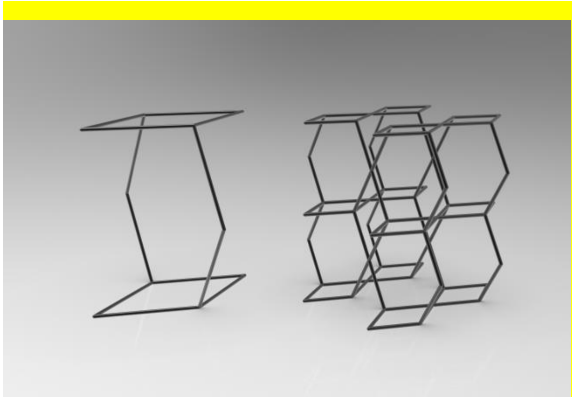

(b) Trans-b

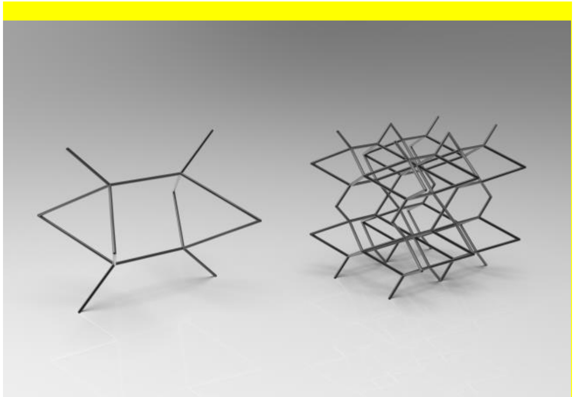

(c) Trans-c

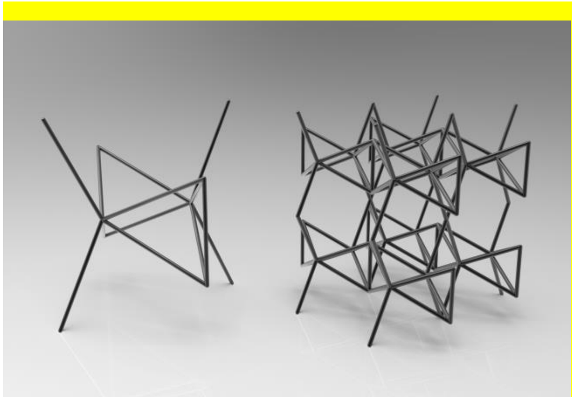

(d) Trans-d

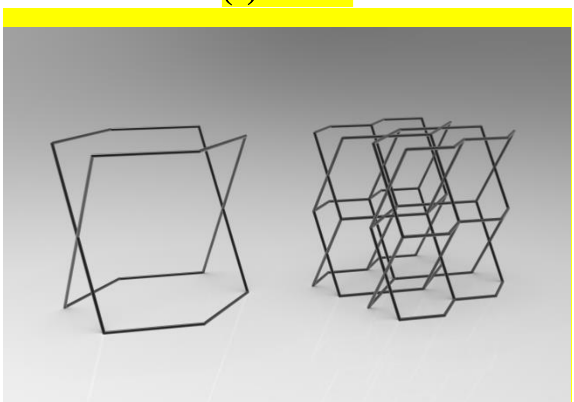

(e) Trans-e

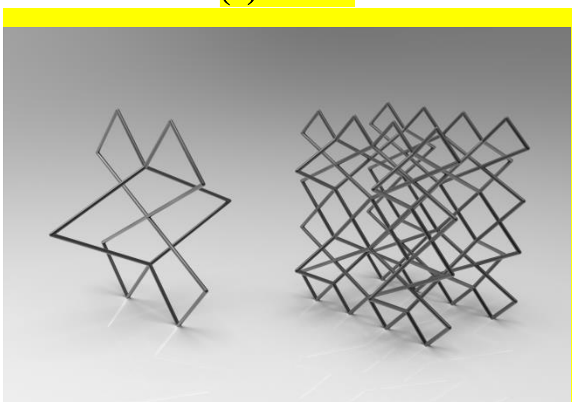

(f) Trans-f

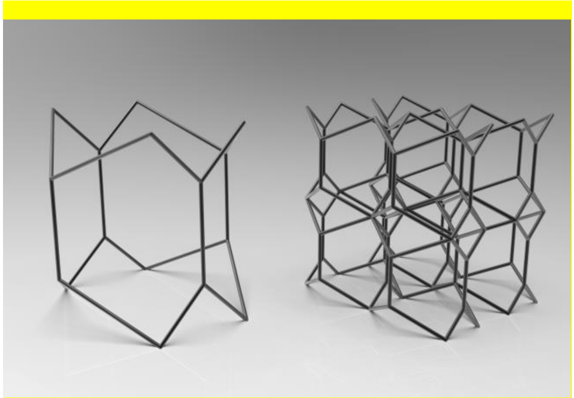

(g) Trans-g

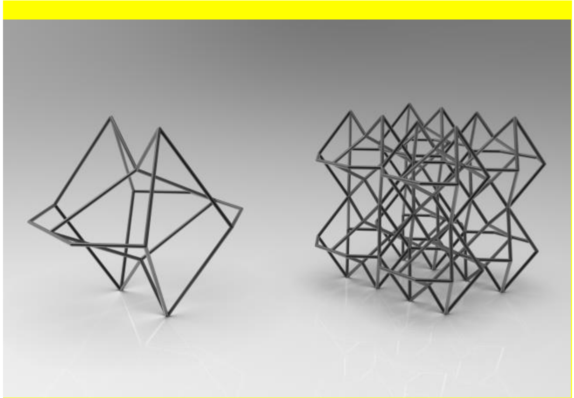

(h) Trans-h

**Fig.9.** Transverse isotropic pentamode lattices

**Table 2.** Effective properties of transverse isotropic pentamode lattices

| | a | b | c | d | e | f | g | h |
|---|---|---|---|---|---|---|---|---|
| $C_{11}$ | 25.582 | 34.109 | 40.349 | 7.323 | 51.163 | 20.417 | 13.287 | 51.102 |
| $C_{22}$ | 25.582 | 8.527 | 40.349 | 29.291 | 12.791 | 45.937 | 53.149 | 22.712 |
| $C_{33}$ | 6.395 | 34.109 | 10.087 | 29.291 | 51.163 | 20.417 | 53.149 | 51.102 |
| $C_{12}$ | 25.582 | 17.054 | 40.349 | 14.646 | 25.582 | 30.625 | 26.574 | 34.068 |
| $C_{13}$ | 12.791 | 34.109 | 20.174 | 14.646 | 51.163 | 20.417 | 26.574 | 51.102 |
| $C_{23}$ | 12.791 | 17.054 | 20.174 | 29.291 | 25.582 | 30.625 | 53.149 | 34.068 |
| $C_{44}$ | 3.29e-5 | 3.29e-5 | 3.44e-5 | 3.29e-5 | 3.37e-5 | 6.65e-5 | 3.37e-5 | 4.28e-5 |
| $C_{55}$ | 3.29e-5 | 3.03e-5 | 3.27e-5 | 4.66e-5 | 3.03e-5 | 3.29e-5 | 3.59e-5 | 3.64e-5 |
| $C_{66}$ | 3.03e-5 | 3.37e-5 | 3.44e-5 | 3.29e-5 | 3.37e-5 | 3.03e-5 | 3.37e-5 | 3.58e-5 |
| $\lambda_{\max\_1}$ | 57.559 | 76.745 | 90.785 | 65.905 | 115.117 | 86.770 | 119.584 | 124.917 |
| $\lambda_{\max\_2}$ | 7.69e-5 | 8.34e-5 | 7.31e-5 | 7.75e-5 | 9.45e-5 | 1.14e-4 | 7.34e-5 | 8.35e-5 |
| $\lambda_{\mathrm{R}}$ | 7.49e5 | 9.20e5 | 1.24e6 | 8.50e5 | 1.22e6 | 7.63e5 | 1.63e6 | 1.50e6 |

Eight orthotropic pentamode lattices are given in Fig.10. The corresponding effective elasticity matrices and eigenvalue ratios are listed in Table 3.

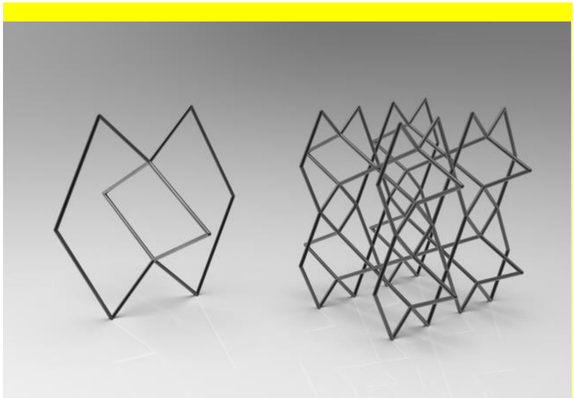

(a) Ortho-a

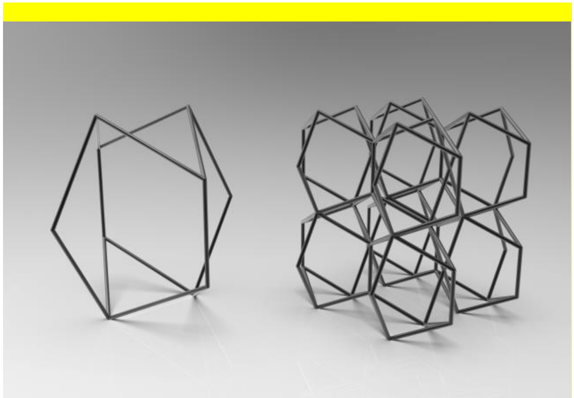

(b) Ortho-b

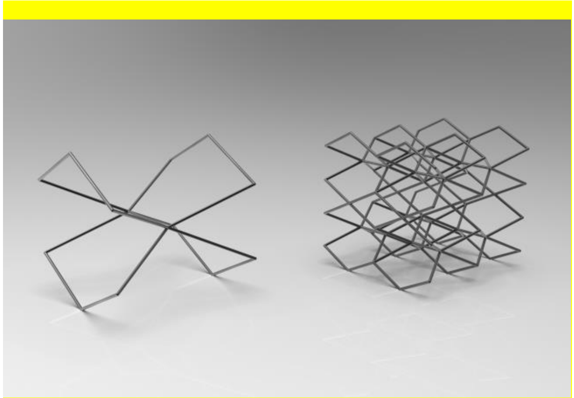

(c) Ortho-c

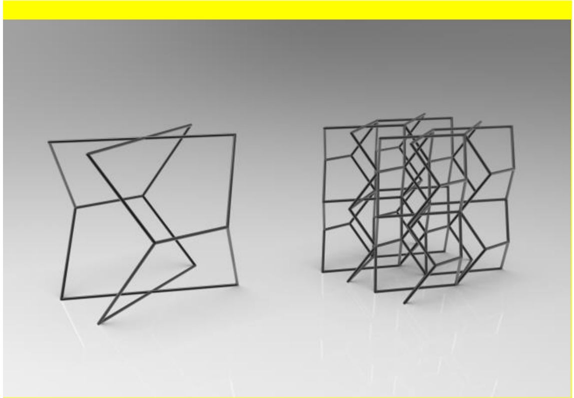

(d) Ortho-d

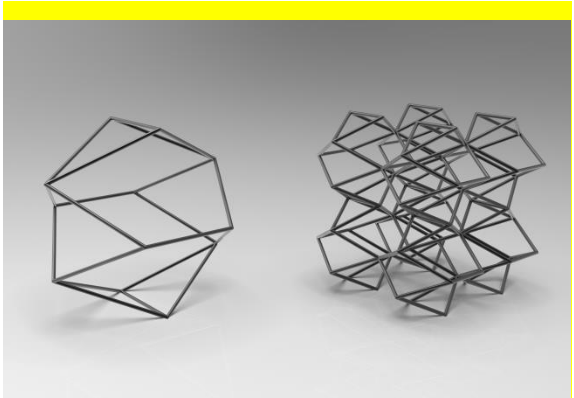

(e) Ortho-e

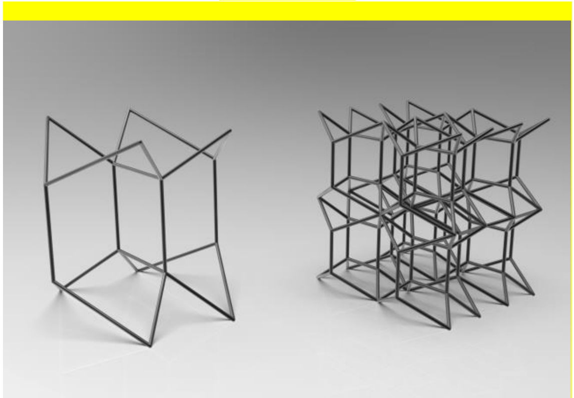

(f) Ortho-f

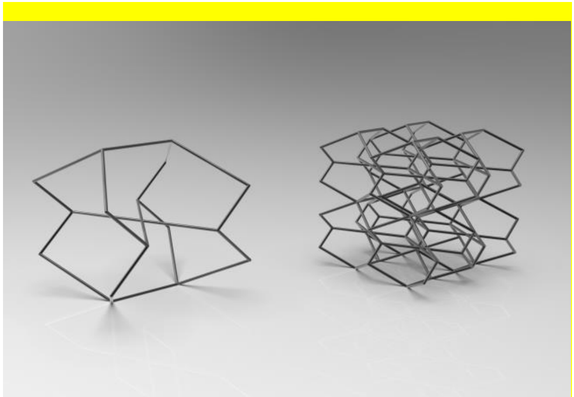

(g) Ortho-g

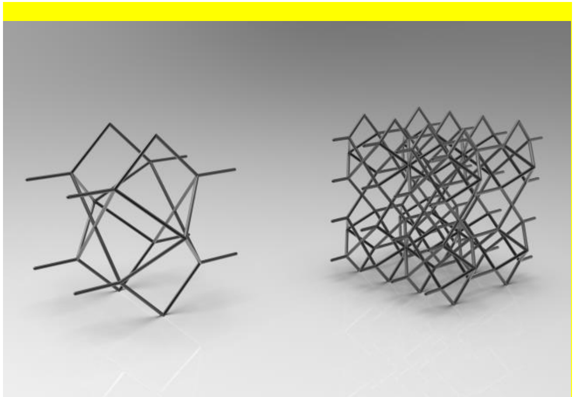

(h) Ortho-h

**Fig.10.** Orthotropic pentamode lattices

**Table 3.** Effective properties of orthotropic pentamode lattices

| | a | b | c | d | e | f | g | h |
|---|---|---|---|---|---|---|---|---|
| $C_{11}$ | 5.677 | 7.323 | 38.291 | 92.337 | 77.083 | 11.046 | 27.313 | 90.835 |
| $C_{22}$ | 22.709 | 29.291 | 86.156 | 10.260 | 34.259 | 99.413 | 109.253 | 10.093 |
| $C_{33}$ | 51.096 | 65.905 | 9.573 | 41.039 | 8.565 | 44.183 | 6.828 | 40.371 |
| $C_{12}$ | 11.355 | 14.646 | 57.437 | 30.779 | 51.389 | 33.138 | 54.626 | 30.278 |
| $C_{13}$ | 17.032 | 21.968 | 19.146 | 61.558 | 25.694 | 22.092 | 13.657 | 60.556 |
| $C_{23}$ | 34.064 | 43.937 | 28.719 | 20.519 | 17.130 | 66.275 | 27.313 | 20.185 |
| $C_{44}$ | 3.29e-5 | 3.29e-5 | 4.39e-5 | 3.37e-5 | 4.39e-5 | 3.48e-5 | 3.37e-5 | 3.44e-5 |
| $C_{55}$ | 4.28e-5 | 4.66e-5 | 3.37e-5 | 3.37e-5 | 4.66e-5 | 3.61e-5 | 3.59e-5 | 3.43e-5 |

| | | | | | | | | |
|---|---|---|---|---|---|---|---|---|
| $C_{66}$ | 3.03e-5 | 3.37e-5 | 3.29e-5 | 4.39e-5 | 3.64e-5 | 4.98e-5 | 3.67e-5 | 3.20e-5 |
| $\lambda_{\max\_1}$ | 79.482 | 102.519 | 134.020 | 143.635 | 119.907 | 154.642 | 143.394 | 141.298 |
| $\lambda_{\max\_2}$ | 8.97e-5 | 8.13e-5 | 8.63e-5 | 8.83e-5 | 8.20e-5 | 7.80e-5 | 8.84e-5 | 8.08e-5 |
| $\lambda_{\mathrm{R}}$ | 8.86e5 | 1.26e6 | 1.55e6 | 1.63e6 | 1.46e6 | 1.98e6 | 1.62e6 | 1.75e6 |

From the above three tables, we can see that the homogenized effective elasticity matrices of these twenty-four lattices all satisfy the requirement of pentamode metamaterials.

*4.2. Stress modes of non-isotropic pentamode lattices*

As mentioned previously, pentamode metamaterials can bear only single mode of stress, which is proportional to the eigenvector corresponding to the non-zero eigenvalue of the elasticity matrix [1]. Here, we name them as stress modes. For non-isotropic pentamode lattices obtained by topology optimization in this paper, their feature is that they can bear load cases proportional to the Eq (16). We will give linear static analysis results of lattices assembled by non-isotropic pentamode lattices to verify that they are stiffer when subjected to the load cases. The lattices Trans-a and Ortho-a are chosen as examples.

The loads and boundary conditions are given in Fig.11. The blue cube represents the bounding box of the lattice structure assembled by $6 \times 6 \times 6$ periodic lattices, measuring 6 mm on one side. For each pair of the opposite faces, the equal magnitude but opposite pressure is uniformly applied. The magnitudes of the resultant forces along each axis are $F_x$, $F_y$ and $F_z$. Due to the symmetry, only one-eighth of the model (i.e., $3 \times 3 \times 3$ lattices) is used in finite element analyses with symmetric boundary conditions. We name the structure assembled by transverse isotropic lattices as the lattice Ⅰ and the structure assembled by orthotropic lattices as the lattice Ⅱ. For all the lattices, the diameters of uniform cylinder bars are 0.02mm. These solid lattices are meshed with linear tetrahedral elements, and the global element seed size is 0.004mm. The Young's modulus for the base material Ti6Al4V is 1.138e5 MPa, and the Poisson's ratio is 0.342.

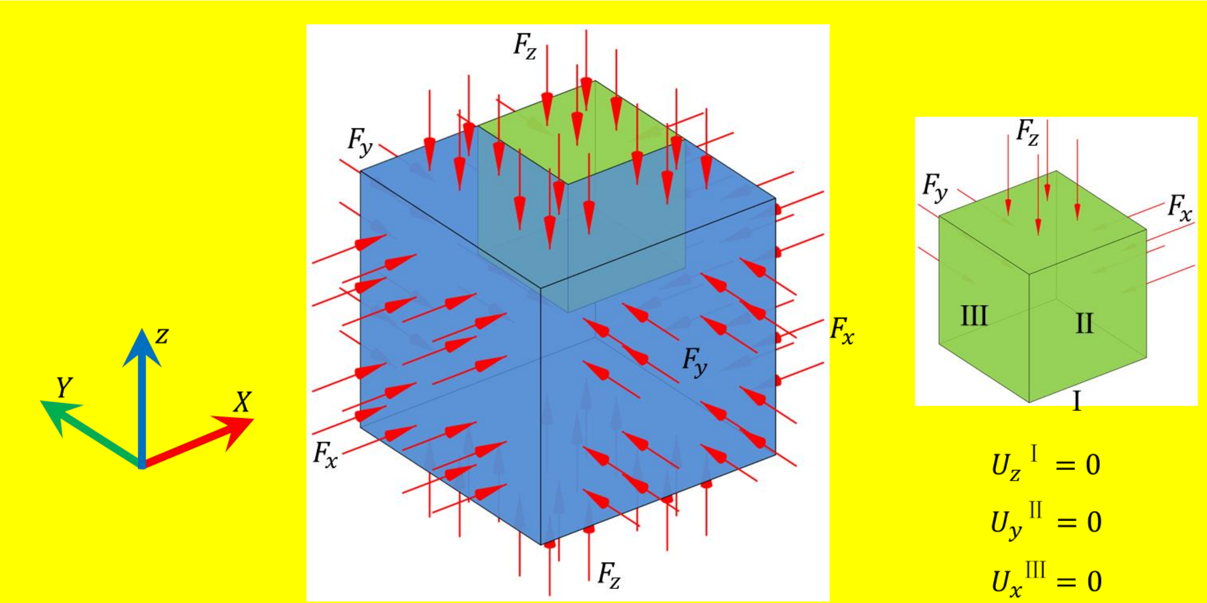


**Fig.11.** Loads and boundary conditions

Six typical load cases applied to each lattice structure are listed in Table 4. The fifth and sixth cases are proportional to the load cases of the transverse isotropic and orthotropic lattices, respectively. The load cases are calculated by the eigenvector of the homogenized effective elasticity matrices of the solid lattices. It is noted that for all these load cases, the vector sum of three forces are the same as 1.73205e-2 N.

**Table 4.** Load cases for the lattices

| | Case 1 | Case 2 | Case 3 | Case 4 | Case 5 | Case 6 |
|---|---|---|---|---|---|---|
| $F_x$ / N | 1.73205e-2 | 0 | 0 | 1.0e-2 | 1.15473e-2 | 4.62887e-3 |
| $F_y$ / N | 0 | 1.73205e-2 | 0 | 1.0e-2 | 1.15474e-2 | 9.24945e-3 |
| $F_z$ / N | 0 | 0 | 1.73205e-2 | 1.0e-2 | 5.77213e-3 | 1.38932e-2 |

The results of linear static finite element analyses using ABAQUS are given below. From Fig.12 and Table 5, we can find that for the lattice Ⅰ, both the displacement magnitude and the total strain energy in the fifth load case are the smallest. From Fig.13 and Table 5, we can also find that for the lattice Ⅱ, both the displacement magnitude and the total strain energy in the sixth load case are the smallest. We emphasize that the total strain energy ratios of the load case to other load cases are considerably small. In one word, a lattice assembled by non-isotropic pentamode lattices is much stiffer when bearing the load case.

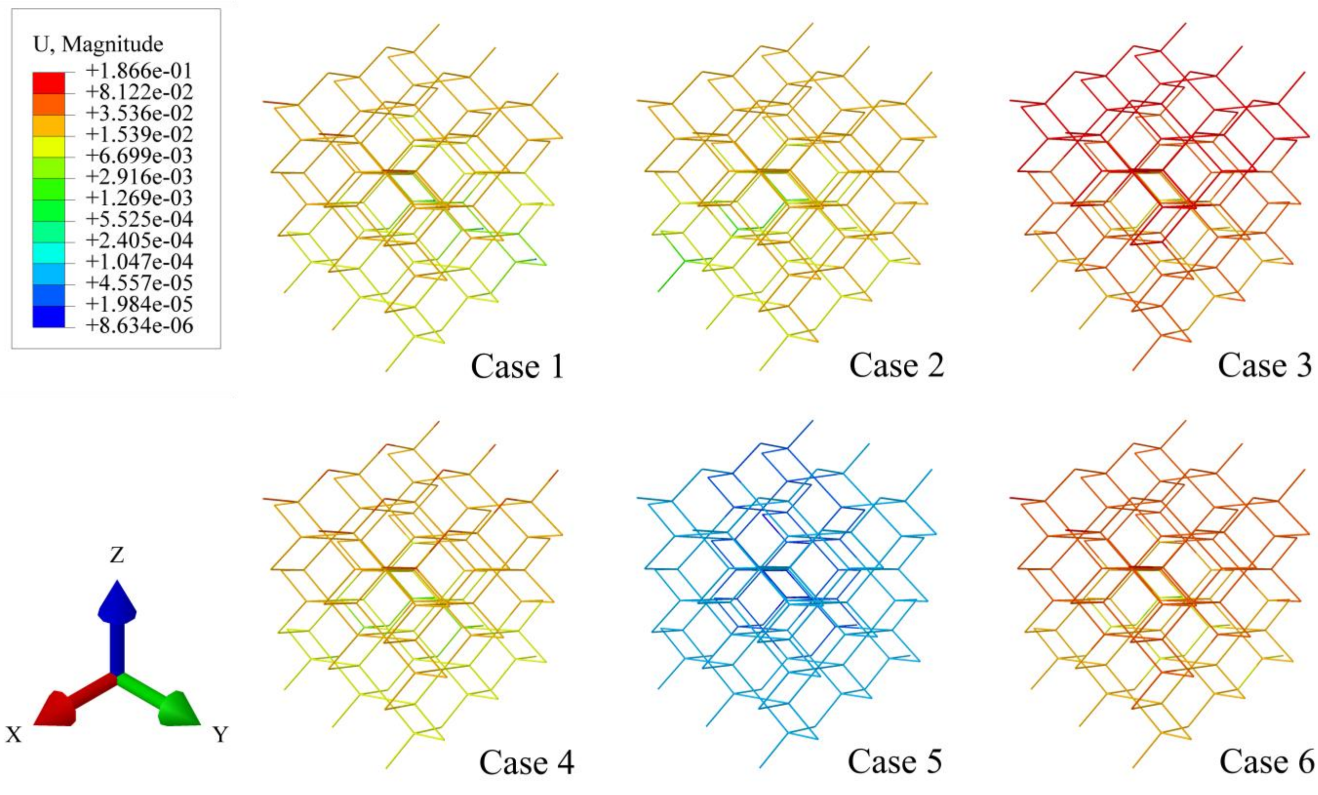


**Fig.12.** Displacement results of the lattice Ⅰ (Unit: mm)

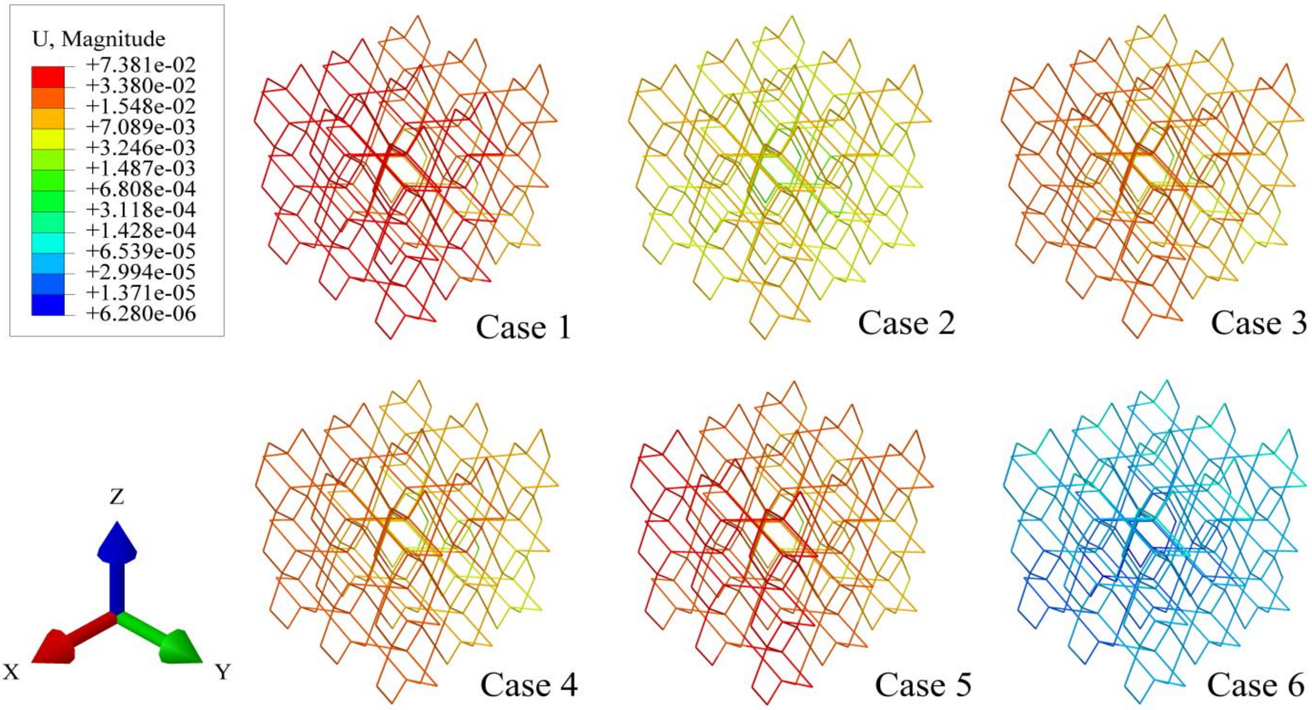


**Fig.13.** Displacement results of the lattice Ⅱ (Unit: mm)

**Table 5.** Total strain energy in different load cases (Unit: mJ)

| | Case 1 | Case 2 | Case 3 | Case 4 | Case 5 | Case 6 |
|---|---|---|---|---|---|---|
| Lattice Ⅰ | 1.51e-4 | 1.34e-4 | 1.14e-3 | 9.61e-5 | 8.77e-7 | 4.25e-4 |
| Lattice Ⅱ | 5.82e-4 | 4.80e-5 | 1.18e-4 | 9.93e-5 | 2.25e-4 | 6.36e-7 |

*4.3. Comparison with conventional diamond-type pentamode lattice*

Here, we will take the new isotropic pentamode lattice Iso-f as an example to compare the static mechanical performance of the new lattices with the conventional diamond-type isotropic pentamode lattice. Like the models in Section 4.2, each lattice used in finite element analyses consists of $3 \times 3 \times 3$ periodic lattices, and symmetric boundary conditions are applied. The values of $F_x$, $F_y$ and $F_z$ are all set to 0.01 N. We name the lattice structure assembled by new isotropic lattices as the lattice Ⅲ, and the lattice structure assembled by diamond-type lattices as the lattice Ⅳ. For the lattice Ⅲ, the diameters of uniform cylinder bars are 0.02mm. For the lattice Ⅳ, the diameters of double-cone bars are $d = 0.02$ mm and $D = 0.0241$ mm. It is noted that the two lattices have the same material volume (0.071 mm$^3$). The mesh and base material properties are the same as models given in Section 4.2.

The linear static analysis results are given in Fig.14 and Fig.15. For the lattice Ⅲ, over 90% of the von Mises stresses of Gauss integration points are between 1.2 MPa and 1.3 MPa, and the ratio of the maximum value to the minimum value is not over 4. The stress distribution in the lattice Ⅲ is relatively uniform. For the lattice Ⅳ, we can see that it suffers from the stress concentration. The maximum von Mises stress of the lattice Ⅳ (146.633 MPa) is much higher than that of the lattice Ⅲ (2.135 MPa).

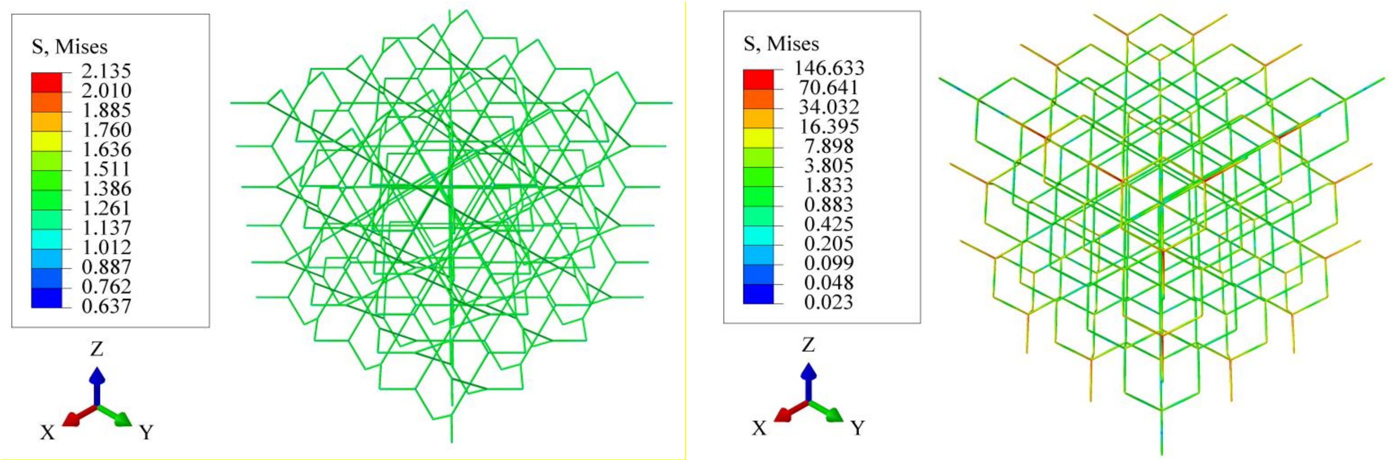


(a) Lattice Ⅲ (b) Lattice Ⅳ

**Fig.14.** Stress results of the lattices (Unit: MPa)

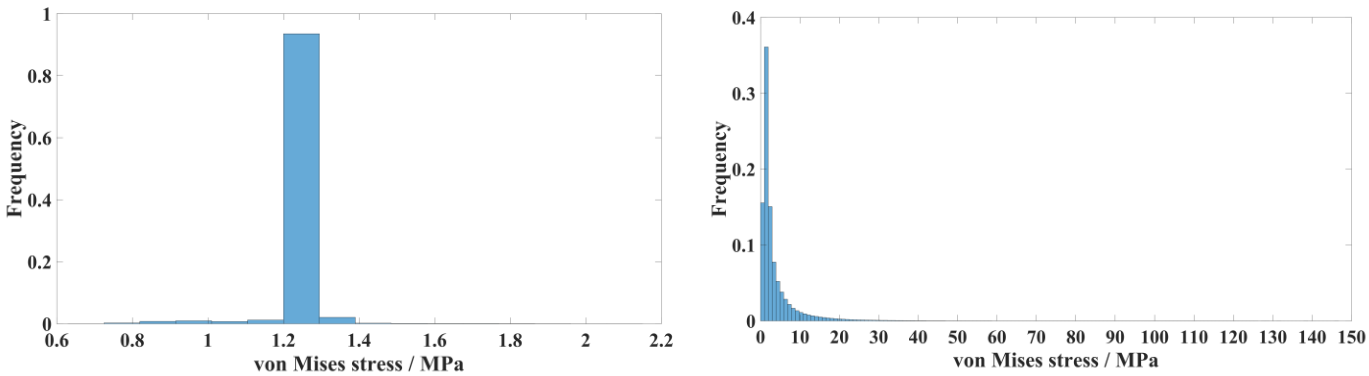


(a) Lattice Ⅲ (b) Lattice Ⅳ

**Fig.15.** Frequency distribution histograms of stress results

The linear buckling analysis results are given in Fig.16. The lowest buckling load of the lattice Ⅲ ($F_x$=$F_y$=$F_z$= 0.253 N) is slightly higher than that of the lattice Ⅳ ($F_x$=$F_y$=$F_z$= 0.241 N). We can see that the first buckling modes of the two lattices all show overall buckling. From the concept of linear static analysis, we can know that when the load is close to $F_x$=$F_y$=$F_z$= 0.253 N, the maximum von Mises stress of the lattice Ⅲ is only 54 MPa. However, for the lattice Ⅳ, even when the load is two-thirds of its lowest buckling load (i.e. $F_x$=$F_y$=$F_z$= 0.1607 N), the maximum von Mises stress theoretically reaches about 2356 MPa and already exceeds the ultimate bearing strength (1860 MPa) of the base material Ti6Al4V. Therefore, no matter the strength or buckling, the lattice Ⅲ can bear much higher hydrostatic stress than the lattice Ⅳ.

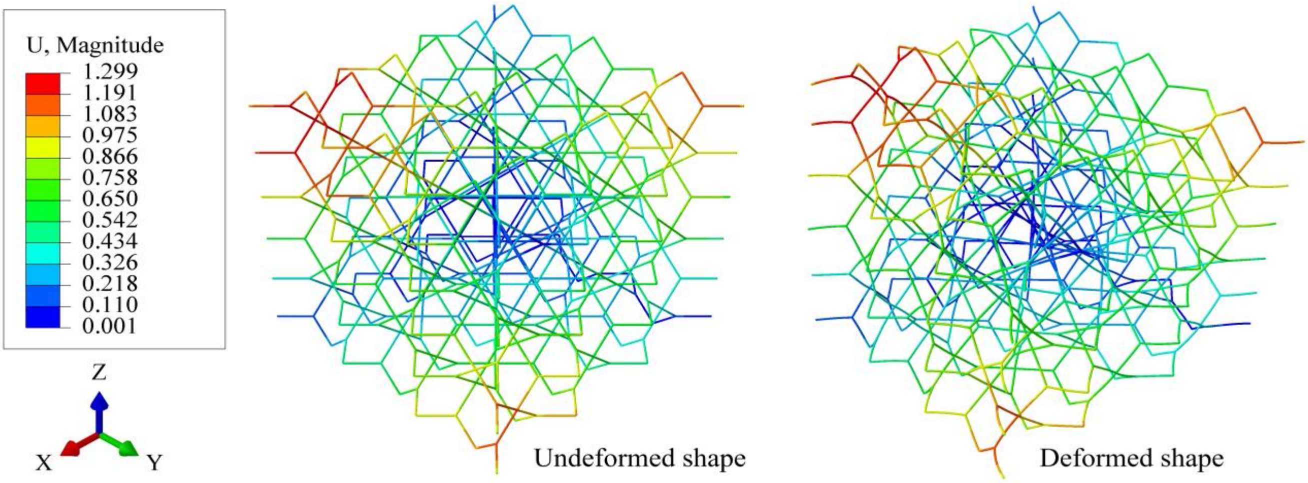


(a) Lattice Ⅲ

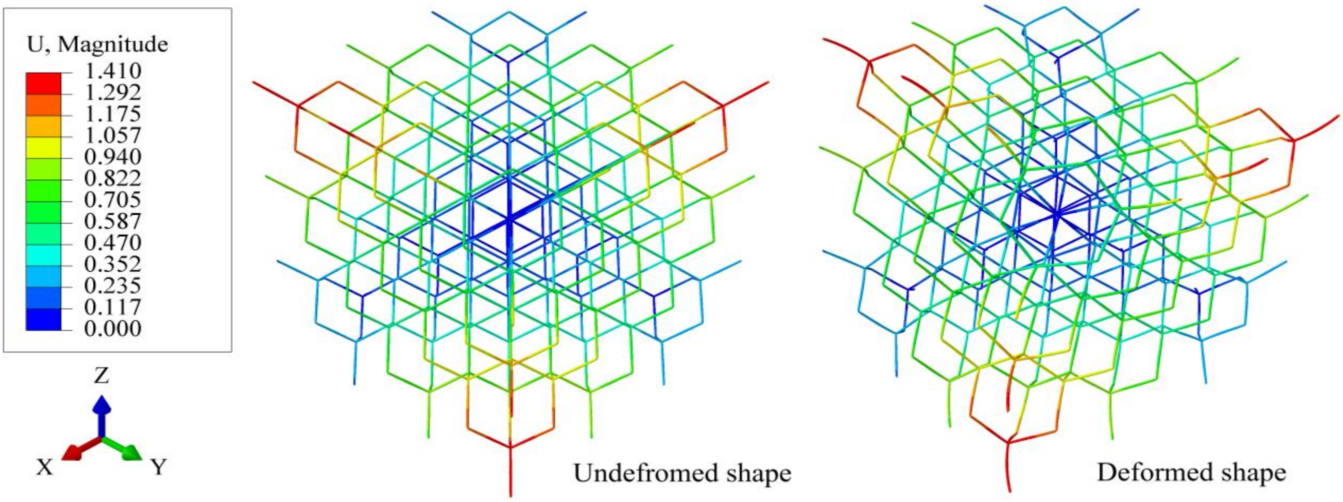


(b) Lattice Ⅳ

**Fig.16.** First buckling modes of the lattices

*4.4. Pentamode lattices with different relative densities*

The proposed design method in this work gives a topologically optimal layout of the solid bars in the space. Based on the optimized skeleton, pentamode lattices with different relative densities can be obtained by changing the geometric dimensions and shapes of the bars. For example, we can introduce the double-cone bars in [3] to replace the uniform cross-section bars, and then change the mid-span diameters $D$ to obtain different relative densities. We emphasize here that other types of structural members rather than double-cone bars can be used to form the pentamode lattices based on the topologically optimized layout.

Take the optimized skeleton shown in Fig.8f as the example. For the lattice in Fig.17a, the diameter of uniform cylinder bars is 0.02mm. Based on the same skeleton, a pentamode lattice using double-cone bars is generated as shown in Fig.17b, of which the diameters are $d = 0.02$ mm and $D = 0.06$ mm. The mesh setting and base material properties are the same as models in Section 4.2.

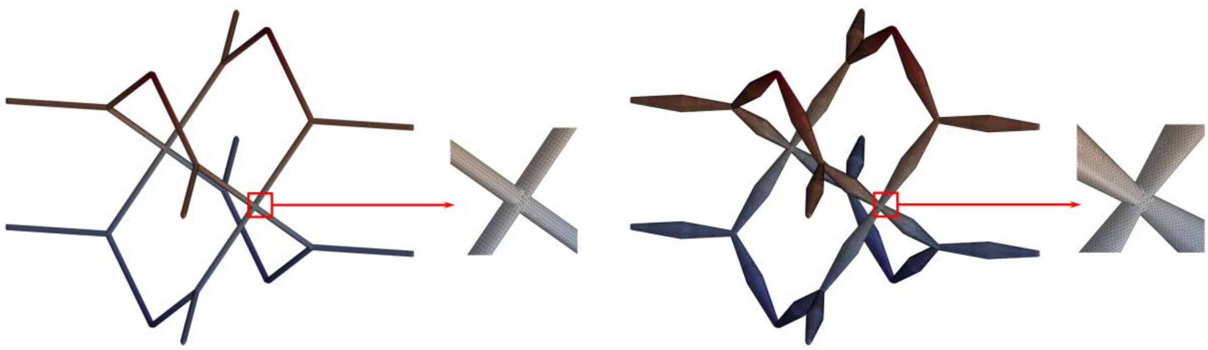

(a) Lattice with lower relative density (b) Lattice with higher relative density

**Fig.17.** Mesh models of pentamode lattices using tetrahedral elements

The effective elasticity matrices, eigenvalue ratios and relative densities $\rho_{\mathrm{R}}$ are listed in Table 6, as below. The unit of elastic constants is MPa.

**Table 6.** Effective properties of pentamode lattices using solid elements

| | a | b |
|---|---|---|
| $C_{11}$ | 33.969 | 108.438 |
| $C_{22}$ | 33.970 | 108.453 |
| $C_{33}$ | 33.970 | 108.453 |
| $C_{12}$ | 33.795 | 107.649 |
| $C_{13}$ | 33.795 | 107.648 |
| $C_{23}$ | 33.796 | 107.656 |
| $C_{44}$ | 0.091 | 0.420 |
| $C_{55}$ | 0.091 | 0.420 |
| $C_{66}$ | 0.091 | 0.420 |
| $\lambda_{\mathrm{max\_1}}$ | 101.561 | 323.750 |
| $\lambda_{\mathrm{max\_2}}$ | 0.175 | 0.797 |
| $\lambda_{\mathrm{R}}$ | 581.864 | 406.004 |
| $\rho_{\mathrm{R}}$ (%) | 0.256 | 1.143 |

From Table 6, we can find that all eigenvalue ratios are relatively large enough to consider these lattices to be pentamode, while the lattices are based on the same skeleton but have different relative densities (0.256% and 1.143%). It is noted that the homogenized shear moduli of the solid structures do not approach to zero, but they are still relatively small enough to allow reasonable pentamode properties.

A micro-lattice (Fig.18) with $2 \times 2 \times 2$ lattices as given in Fig.17b is prototyped using the Digital Light Processing (DLP) technique, with Octave Light R1 machine using a rubber-like material (TangoGray FLX950), as shown in Fig.19.

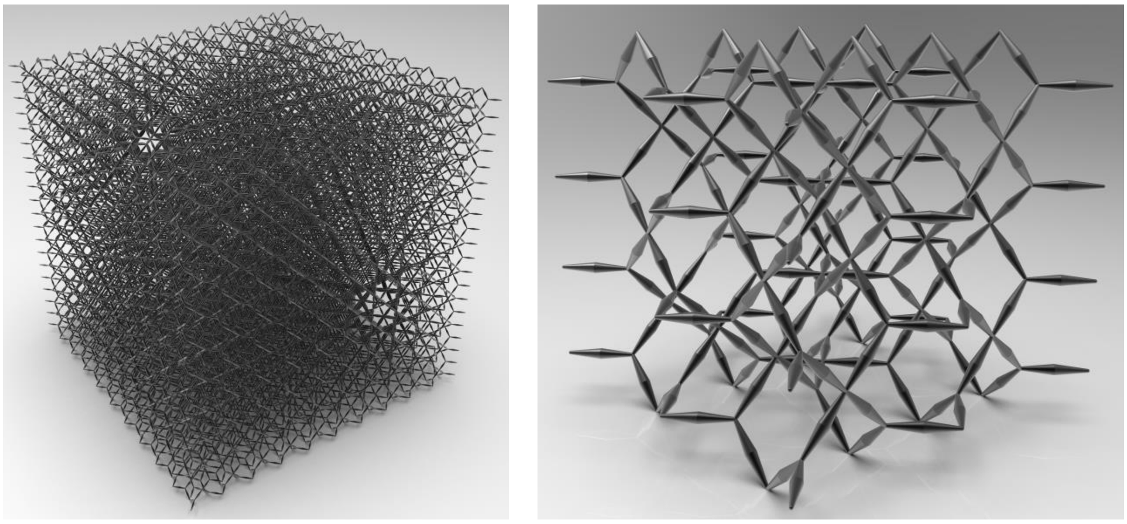

(a) $10 \times 10 \times 10$ (b) $2 \times 2 \times 2$

**Fig.18.** Periodic arrays of the pentamode lattices

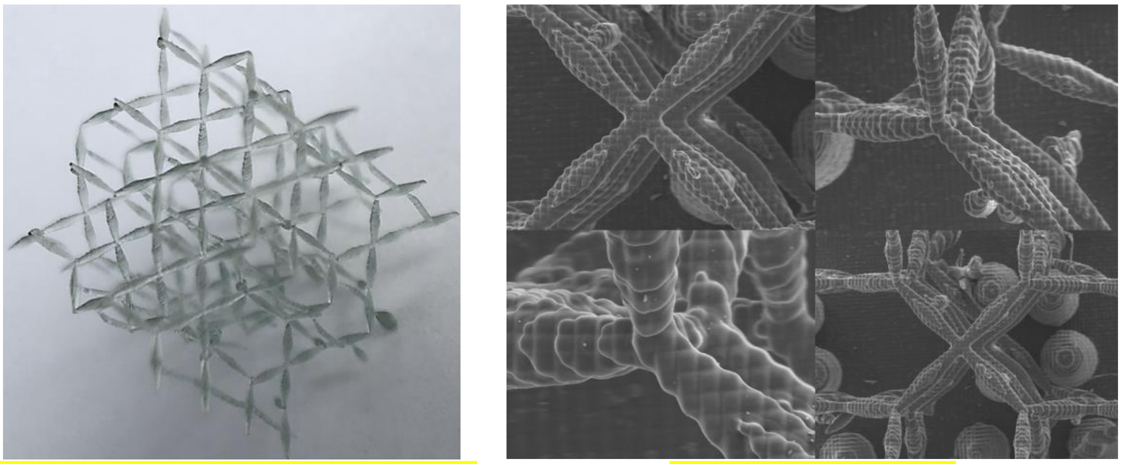

(a) Additively manufactured specimen (b) Microscopic photo

**Fig.19.** An additively manufactured micro-lattice with $2 \times 2 \times 2$ lattices

## 5. Conclusions

This work has derived the necessary and sufficient condition required for elasticity constants of pentamode metamaterials with at least orthotropic symmetry. We found that a large ratio of the bulk modulus to the shear modulus is no more a sufficient condition for non-isotropic pentamode metamaterials. A ground structure method with the genetic algorithm is then proposed to conduct topology optimization of pentamode metamaterials with at least orthotropic symmetry. Geometric constraints on intersection and overlap of bars are applied to the lattice with a new efficient detection method to obtain realistic designs. Twenty-four new pentamode lattices without intersection or overlap of bars are discovered, including isotropic, transverse isotropic and orthotropic ones. The optimization results have demonstrated the effectiveness and efficiency of the proposed design method. The further analyses have verified that lattices assembled by non-isotropic pentamode lattices are much stiffer when subjected to their bearable load cases. From the comparative analysis results, we can see that one isotropic pentamode lattice obtained by topology optimization can form lattices to bear much higher hydrostatic stress than the conventional diamond-type pentamode lattice.

Moreover, we propose that based on the optimized skeleton, pentamode lattices with different relative densities can be obtained just by changing the geometric dimensions and shapes of the bars.

In the future, we will further derive the necessary and sufficient condition required for elasticity constants of fully anisotropic pentamode lattices, and modify the mathematical optimization model based on the derived condition. Then the topology optimization design framework proposed in this paper can also be used to find new fully anisotropic pentamode lattices with minor modifications. Moreover, potential applications of the new pentamode lattices on cloaking devices will also be our next study.

## Acknowledgements

This work was partially supported by the Australian Research Council (ARC) - Discovery Projects (DP210101353). This work particularly thanks for Prof Bo Sun and his team in additive manufacturing of the pentamode lattice and Mr. Weihong Dong for his help in 3D renderings.

## References

[1] G.W. Milton, A. V. Cherkaev, Which elasticity tensors are realizable?, J. Eng. Mater. Technol. Trans. ASME. 117 (1995) 483–493. https://doi.org/10.1115/1.2804743.

[2] G.W. Milton, M. Briane, J.R. Willis, On cloaking for elasticity and physical equations with a transformation invariant form, New J. Phys. 8 (2006) 248. https://doi.org/10.1088/1367-2630/8/10/248.

[3] M. Kadic, T. Bückmann, N. Stenger, M. Thiel, M. Wegener, On the practicability of pentamode mechanical metamaterials, Appl. Phys. Lett. 100 (2012) 191901. https://doi.org/10.1063/1.4709436.

[4] C. Cai, Z. Wang, Q. Li, Z. Xu, X. Tian, Pentamode metamaterials with asymmetric double-cone elements, J. Phys. D. Appl. Phys. 48 (2015) 175103. https://doi.org/10.1088/0022-3727/48/17/175103.

[5] Y. Huang, X. Lu, G. Liang, Z. Xu, Pentamodal property and acoustic band gaps of pentamode metamaterials with different cross-section shapes, Phys. Lett. Sect. A Gen. At. Solid State Phys. 380 (2016) 1334–1338. https://doi.org/10.1016/j.physleta.2016.01.041.

[6] A.N. Norris, Acoustic metafluids, J. Acoust. Soc. Am. 125 (2009) 839–849. https://doi.org/10.1121/1.3050288.

[7] R. Schittny, T. Bückmann, M. Kadic, M. Wegener, Elastic measurements on macroscopic three-dimensional pentamode metamaterials, Appl. Phys. Lett. 103 (2013) 231905. https://doi.org/10.1063/1.4838663.

[8] R. Hedayati, A.M. Leeflang, A.A. Zadpoor, Additively manufactured metallic pentamode meta-materials, Appl. Phys. Lett. 110 (2017) 91905. https://doi.org/10.1063/1.4977561.

[9] A.N. Norris, Acoustic cloaking theory, Proc. R. Soc. A Math. Phys. Eng. Sci. 464 (2008) 2411–2434. https://doi.org/10.1098/rspa.2008.0076.

[10] N.H. Gokhale, J.L. Cipolla, A.N. Norris, Special transformations for pentamode acoustic cloaking, J. Acoust. Soc. Am. 132 (2012) 2932–2941. https://doi.org/10.1121/1.4744938.

[11] C.N. Layman, C.J. Naify, T.P. Martin, D.C. Calvo, G.J. Orris, Highly anisotropic elements for acoustic

pentamode applications, Phys. Rev. Lett. 111 (2013) 24302. https://doi.org/10.1103/PhysRevLett.111.024302.

[12] Y. Chen, X. Liu, G. Hu, Latticed pentamode acoustic cloak, Sci. Rep. 5 (2015) 15745. https://doi.org/10.1038/srep15745.

[13] Y. Guo, T. Dekorsy, M. Hettich, Topological guiding of elastic waves in phononic metamaterials based on 2D pentamode structures, Sci. Rep. 7 (2017) 18043. https://doi.org/10.1038/s41598-017-18394-8.

[14] Z. Sun, H. Jia, Y. Chen, Z. Wang, J. Yang, Design of an underwater acoustic bend by pentamode metafluid, J. Acoust. Soc. Am. 143 (2018) 1029–1034. https://doi.org/10.1121/1.5024351.

[15] A.O. Krushynska, P. Galich, F. Bosia, N.M. Pugno, S. Rudykh, Hybrid metamaterials combining pentamode lattices and phononic plates, Appl. Phys. Lett. 113 (2018) 201901. https://doi.org/10.1063/1.5052161.

[16] T. Bückmann, M. Thiel, M. Kadic, R. Schittny, M. Wegener, An elasto-mechanical unfeelability cloak made of pentamode metamaterials, Nat. Commun. 5 (2014) 4130. https://doi.org/10.1038/ncomms5130.

[17] L. Hai, Q. Zhao, Y. Meng, Unfeelable Mechanical Cloak Based on Proportional Parameter Transform in Bimode Structures, Adv. Funct. Mater. 28 (2018) 1801473. https://doi.org/10.1002/adfm.201801473.

[18] F. Fabbrocino, A. Amendola, G. Benzoni, F. Fraternali, Seismic application of pentamode lattices, Ing. Sismica. 33 (2016) 62–70.

[19] G.F. Méjica, A.D. Lantada, Comparative study of potential pentamodal metamaterials inspired by Bravais lattices, Smart Mater. Struct. 22 (2013) 115013. https://doi.org/10.1088/0964-1726/22/11/115013.

[20] B. Xu, Five kinds of micro-structures of pentamode metamaterials and their performance analysis, Dalian University of Technology, 2015.

[21] Q. Li, J.S. Vipperman, Three-dimensional pentamode acoustic metamaterials with hexagonal lattices, J. Acoust. Soc. Am. 145 (2019) 1372–1377. https://doi.org/10.1121/1.5093622.

[22] Y. Huang, X. Zhang, M. Kadic, G. Liang, Stiffer, stronger and centrosymmetrical class of pentamodal mechanical metamaterialss, Materials. 12 (2019) 3470. https://doi.org/10.3390/ma12213470.

[23] M. Kadic, T. Bückmann, R. Schittny, M. Wegener, On anisotropic versions of three-dimensional pentamode metamaterials, New J. Phys. 15 (2013) 23029. https://doi.org/10.1088/1367-2630/15/2/023029.

[24] G.W. Milton, M. Briane, D. Harutyunyan, On the possible effective elasticity tensors of 2-dimensional and 3-dimensional printed materials, Math. Mech. Complex Syst. 5 (2017) 41–94. https://doi.org/10.2140/memocs.2017.5.41.

[25] E. Andreassen, B.S. Lazarov, O. Sigmund, Design of manufacturable 3D extremal elastic microstructure, Mech. Mater. 69 (2014) 1–10. https://doi.org/10.1016/j.mechmat.2013.09.018.

[26] J. Wu, Z. Luo, H. Li, N. Zhang, Level-set topology optimization for mechanical metamaterials under hybrid uncertainties, Comput. Methods Appl. Mech. Eng. 319 (2017) 414–441. https://doi.org/10.1016/j.cma.2017.03.002.

[27] H. Li, Z. Luo, L. Gao, P. Walker, Topology optimization for functionally graded cellular composites with metamaterials by level sets, Comput. Methods Appl. Mech. Eng. 328 (2018) 340–364. https://doi.org/10.1016/j.cma.2017.09.008.

[28] Y.M. Xie, X. Yang, J. Shen, X. Yan, A. Ghaedizadeh, J. Rong, X. Huang, S. Zhou, Designing orthotropic materials for negative or zero compressibility, Int. J. Solids Struct. 51 (2014) 4038–4051. https://doi.org/10.1016/j.ijsolstr.2014.07.024.

[29] O. Sigmund, Materials with prescribed constitutive parameters: An inverse homogenization problem, Int. J. Solids Struct. 31 (1994) 2313–2329. https://doi.org/10.1016/0020-7683(94)90154-6.

[30] O. Sigmund, Tailoring materials with prescribed elastic properties, Mech. Mater. 20 (1995) 351–368. https://doi.org/10.1016/0167-6636(94)00069-7.

[31] F. Wang, O. Sigmund, J.S. Jensen, Design of materials with prescribed nonlinear properties, J. Mech. Phys. Solids. 69 (2014) 156–174. https://doi.org/10.1016/j.jmps.2014.05.003.

[32] J. Yvonnet, Computational Homogenization of Heterogeneous Materials with Finite Elements, 1st ed., Springer, Cham, 2019. https://doi.org/10.1007/978-3-030-18383-7.

[33] The MathWorks, Global Optimization Toolbox, (2019). https://www.mathworks.com/help/gads/.

[34] T. Zegard, G.H. Paulino, GRAND3 — Ground structure based topology optimization for arbitrary 3D domains using MATLAB, Struct. Multidiscip. Optim. 52 (2015) 1161–1184. https://doi.org/10.1007/s00158-015-1284-2.

[35] M. Ohsaki, N. Katoh, Topology optimization of trusses with stress and local constraints on nodal stability and member intersection, Struct. Multidiscip. Optim. 29 (2005) 190–197. https://doi.org/10.1007/s00158-004-0480-2.

[36] H. Cui, H. An, H. Huang, Truss topology optimization considering local buckling constraints and restrictions on intersection and overlap of bar members, Struct. Multidiscip. Optim. 58 (2018) 575–594. https://doi.org/10.1007/s00158-018-1910-x.

[37] P. Bourke, The shortest line between two lines in 3D, (1998). http://paulbourke.net/geometry/pointlineplane/.

# Topological Design of Pentamode Lattice Metamaterials Using A Ground Structure Method

Zuyu Li [a], Zhen Luo [a,*], Lai-Chang Zhang [b], Chun-Hui Wang [c]

[a] School of Mechanical and Mechatronic Engineering
University of Technology Sydney, Sydney, NSW 2007, Australia
*( [*]Corresponding authors: zhen.luo@uts.edu.au, A/Prof Zhen Luo)*

[b] School of Engineering
Edith Cowan University, Perth, WA 6027, Australia

[c] School of Mechanical and Manufacturing Engineering
University of New South Wales, Sydney, NSW 2052, Australia

---

## Statement of Authors' Contribution

This paper is about topological optimization of lattice microarchitectures of solid pentamode materials with at least elastically orthotropic symmetry. The detailed contributions of all authors are stated as follows:

The first author, **Zuyu Li** is a PhD candidate, who mainly completed the coding of all the algorithms and numerical implementation of the proposed optimization method, as well as the writing of the draft of this paper. Zuyu has made solid contribution to the detailed implementation of all the research tasks.

The second author, **Dr Zhen Luo**, is the principal supervisor and also the corresponding author of this paper. He is responsible for the whole this research project that is in financially funded by the ARC (Australian Research Council) - Discovery project. Dr Zhen Luo is the leading core investigator of the govement project.

Dr Luo contributes the originality of the research ideas, supervision of the research progress of all components and paragraphs of this paper, the accuracy and correctness of the data (modelling, simulation, analysis, design optimization and manufacturing) in this paper, as well as editing of the whole paper, and submission of the paper for reviewing. Dr Luo has made a solid contribution to the overall technical aspects of this paper.

The third author, **Prof Laichang Zhang** mainly contributed to the prototyping of the optimized design, and numerical validation of the designed specimen.

The fourth author, **Prof Chun-Hui Wang** mainly contributed to the material behavior of pentamodel materials, as well as a reasonable engagement of the derivation of the sufficient and necessary condition.

**Declaration of interests**

☒ The authors declare that they have no known competing financial interests or personal relationships that could have appeared to influence the work reported in this paper.

☐The authors declare the following financial interests/personal relationships which may be considered as potential competing interests: